

# Symptomatic Features of Intraplate Earthquakes

Abhijit Gangopadhyay and Pradeep Talwani

Department of Geological Sciences, University of South Carolina

## ABSTRACT

Available geological, geophysical, and seismological data for 39 cases were compared and analyzed to understand the cause of intraplate earthquakes. The results revealed common features which can be used to test models for their seismogenesis. Intraplate seismicity occurs in the vicinity of "stress concentrators" within pre-existing zones of weakness, most commonly failed rifts. These stress concentrators are structures where plate tectonic stresses can cause a localized build-up of stresses and, ultimately, earthquakes. These include intersecting faults, buried plutons, and rift pillows. One of the intersecting faults was often found to be tens of kilometers in length and oriented optimally with respect to the maximum horizontal stress direction. Intraplate earthquakes have longer return periods compared to their plate-boundary counterparts. They occur in failed rifts of all ages, whereas those not associated with rifts occur only in the Precambrian crust. The former have shorter return periods ( $\leq 500$  years) compared to the latter (thousands of years).

## INTRODUCTION

Intraplate earthquakes occur in plates that are characterized by very low strain rates (Johnston, 1989; Johnston *et al.*, 1994). Although their potential for widespread destruction is large, intraplate earthquakes occur less frequently compared to their plate-boundary counterparts. Primarily because of their rarity and a general absence of accompanying surface ruptures, their mechanisms are not well understood. In this paper we expand Johnston's (1989) definition of stable continental regions (SCR) to include Cenozoic-age structures and refer to them collectively as intraplate regions. To understand their seismogenesis we have used a two-step approach. The first step, the subject of this paper, is a global synthesis of

available geological, geophysical, and seismological data for intraplate earthquakes, to seek diagnostic and characteristic features. The second step, not addressed here, is to build simple mechanical models to evaluate the roles of these characteristic features in the generation and location of seismicity. Before we present our analyses of global data we review earlier explanations of intraplate seismicity.

## REVIEW OF MODELS FOR INTRAPLATE EARTHQUAKES

Earlier studies have described several characteristic features of intraplate earthquakes but not their genesis (Sykes, 1978; Johnston, 1989; Talwani, 1989; Talwani and Rajendran, 1991; Zoback, 1992; Johnston *et al.*, 1994). An observed spatial association of intraplate earthquakes with mafic bodies and analytical computations led to suggestions of causal association (Simmons *et al.*, 1976; Kane, 1977; Long and Champion, 1977; Campbell, 1978; McKeown, 1978; Barstow *et al.*, 1981). Other studies (Talwani *et al.*, 1979; Illies, 1982; King and Nabelek, 1985; King, 1986; Talwani, 1988) noted that these earthquakes could be associated with stress build-up near kinks and intersections, as was also shown by numerical analyses (Andrews 1989, 1994). To explain the deep earthquakes in the Amazonas rift basin, Zoback and Richardson (1996) suggested stress perturbation on a buried rift pillow in the lower crust. A high-density intrusion into the lower continental crust is referred to as a "rift pillow" (Zoback and Richardson, 1996) or a "stress pillow" (Singh and Meissner, 1995). The same concept was applied to earthquakes in the New Madrid seismic zone (NMSZ) and to the Jabalpur earthquake in India by Stuart *et al.* (1997) and Rajendran and Rajendran (1998, 1999), respectively. Other proposed models include the deglaciation model (Basham *et al.*, 1977; Stein *et al.*, 1979), gravitationally induced stresses

at structural boundaries (Goodacre and Hasegawa, 1980), and reduction of strength of rocks by mechanical or chemical means (Talwani and Acree, 1984; Costain *et al.*, 1987).

Three recent models have also been proposed to explain intraplate earthquakes. Kenner and Segall (2000) proposed a time-dependent mechanical model for the generation of repeated large intraplate earthquakes. Their model requires a weak lower crustal zone embedded within the elastic lithosphere and includes stress-controlled coseismic rupture and postseismic perturbations to the deformation field. In a model proposed by Thybo *et al.* (2000), the cause of intraplate earthquakes is attributed to a seismically defined lateral transition in the upper mantle. Pollitz *et al.* (2001) proposed a geodynamic model for stress concentration and applied it to NMSZ. They suggested that a mafic body located in the deep crust beneath the seismically active region of NMSZ started sinking due to a perturbation field such as that provided by the effect of deglaciation (Grollmund and Zoback, 2001), thus suddenly weakening the lower crust. The downward pull

exerted by the mafic body flexes or breaks the upper crust, resulting in earthquakes. The cycle repeats itself with continued sinking of the mafic body. They assume that thrust faulting is the primary type of faulting at NMSZ, as also suggested by Johnston (1996) and Hough *et al.* (2000). To assess these models we decided to critically examine the global database pertaining to intraplate seismicity.

## CASE HISTORIES OF EXAMINED INTRAPLATE REGIONS

We examined 20 case histories of intraplate regions related to 39 earthquakes of  $M \geq 5.0$  or greater. They are listed chronologically in Table 1. Several analytical studies have shown that geologic features such as intersecting faults, buried plutons, and rift pillows are capable of localizing stress (Campbell, 1978; King and Nabelek, 1985; King, 1986; Zoback and Richardson, 1996). We have labeled these structures "stress concentrators", *i.e.*, these are the locations where plate tec-

**TABLE 1**  
Examined Intraplate Regions

Major Earthquake	Date (MM/DD/YYYY)	Associated Intraplate Region	Magnitude	References
Basel	10/18/1356	Upper Rhine Graben, Switzerland	$M_w$ 6.0–6.5	Lemeille <i>et al.</i> (1999); Meghraoui <i>et al.</i> (2001)
Charlevoix	02/05/1663	St. Lawrence Rift, Canada	$M_w$ 7.0±0.5	Ebel (1996)
Charlevoix	02/06/1663	St. Lawrence Rift, Canada	$M_w$ >5.0	Ebel (1996)
Charlevoix	02/06/1663	St. Lawrence Rift, Canada	$M_w$ >5.0	Ebel (1996)
Charlevoix	02/06/1663	St. Lawrence Rift, Canada	$M_w$ >5.0	Ebel (1996)
Charlevoix	02/07/1663	St. Lawrence Rift, Canada	$M_w$ >5.0	Ebel (1996)
New Madrid	12/16/1811	New Madrid Seismic Zone, USA	$M_w$ 8.1	Johnston (1996)
New Madrid	01/23/1812	New Madrid Seismic Zone, USA	$M_w$ 7.8	Johnston (1996)
New Madrid	02/07/1812	New Madrid Seismic Zone, USA	$M_w$ 8.0	Johnston (1996)
Kutch	1819	Kachchh Rift Basin, India	$M_w$ 7.8	Johnston <i>et al.</i> (1994)
Charleston	08/31/1886	Middleton Place-Summerville Seismic Zone, USA	$M_w$ 7.3	Johnston (1996)
Belle Prairie, Illinois	09/27/1891	Illinois Basin, USA	$m_b$ 5.8	Kolata and Hildenbrand (1997)
Swabian Jura	11/16/1911	Swabian Jura, southwest Germany	$M_w$ 6.1	Turnovsky and Schneider (1982)
Charlevoix	03/01/1925	St. Lawrence Rift, Canada	$M_w$ 6.0 - 6.5	Bent (1992)
Son Valley	1927	Narmada Rift Basin, India	$m_b$ 6.5	Gupta <i>et al.</i> (1997); Rajendran and Rajendran (1998)
Satpura	1938	Narmada Rift Basin, India	$m_b$ 6.3	Rajendran and Rajendran (1998)
Accra	1939	Ghana	$M_w$ 6.5	Talwani and Rajendran (1991)
Swabian Jura	05/28/1943	Swabian Jura, southwest Germany	$M_S$ 5.2	Schneider (1979)
Anjar	07/21/1956	Kachchh Rift Basin, India	$M_w$ 6.0	Chung and Gao (1995)
Amazonas	12/14/1963	Amazonas Rift Basin, Brazil	$m_b$ 5.1	Assumpcao and Suarez (1988)
Xingtai	03/06/1966	North China Rift Basin, China	$M_w$ 7.3	Talwani and Rajendran (1991)
Meckering	10/14/1968	Australian Craton (west), Australia	$M_S$ 6.8	Langston (1987)

**TABLE 1 (Continued)**  
**Examined Intraplate Regions**

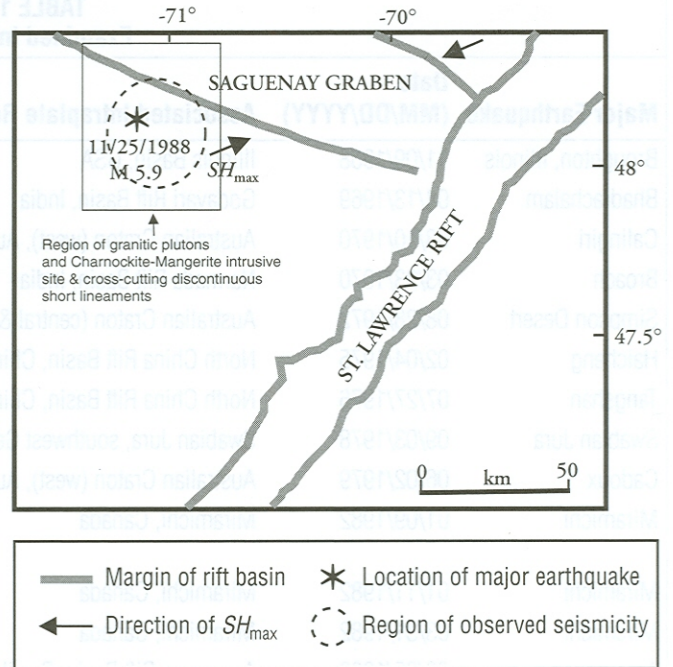
<b>Major Earthquake</b>	<b>Date (MM/DD/YYYY)</b>	<b>Associated Intraplate Region</b>	<b>Magnitude</b>	<b>References</b>
Broughton, Illinois	11/09/1968	Illinois Basin, USA	$m_b$ 5.5	Kolata and Hildenbrand (1997)
Bhadrachalam	04/13/1969	Godavari Rift Basin, India	$M_w$ 5.7	Chung (1993)
Calingiri	03/10/1970	Australian Craton (west), Australia	$M_S$ 5.1	Denham (1988)
Broach	03/23/1970	Narmada Rift Basin, India	$M_w$ 5.4	Chung (1993)
Simpson Desert	08/28/1972	Australian Craton (central & east), Australia	$M_w$ 5.6	Talwani and Rajendran (1991)
Haicheng	02/04/1975	North China Rift Basin, China	$M_w$ 7.3	Talwani and Rajendran (1991)
Tangshan	07/27/1976	North China Rift Basin, China	$M_S$ 7.8	Nabelek <i>et al.</i> (1987)
Swabian Jura	09/03/1978	Swabian Jura, southwest Germany	$M_S$ 5.1	Turnovsky and Schneider (1982)
Cadoux	06/02/1979	Australian Craton (west), Australia	$M_S$ 6.0	Denham (1988)
Miramichi	01/09/1982	Miramichi, Canada	$M_w$ 5.7, 5.1	Hasegawa (1991); Talwani and Rajendran (1991)
Miramichi	01/11/1982	Miramichi, Canada	$M_w$ 5.4	Hasegawa (1991)
Miramichi	03/31/1982	Miramichi, Canada	$M_w$ 5.0	Hasegawa (1991)
Amazonas	08/05/1983	Amazonas Rift Basin, Brazil	$m_b$ 5.5	Assumpção and Suarez (1988)
Tasman Sea	11/25/1983	Australian Craton (central & east), Australia	$M_w$ 5.8	Talwani and Rajendran (1991)
Guinea	12/22/1983	Guinea	$M_w$ 6.4	Talwani and Rajendran (1991)
Marryat Creek	03/30/1986	Australian Craton (central & east), Australia	$M_S$ 5.8	Denham (1988)
Southern Illinois	06/10/1987	Illinois Basin, USA	$m_b$ 5.2	McBride <i>et al.</i> (2002)
Tennant Creek	01/22/1988	Australian Craton (central & east), Australia	$M_S$ 6.3, 6.4, 6.7	Bowman (1991); Bowman (1992)
Saguenay	11/25/1988	Saguenay Graben, Canada	$m_b$ 5.9	Du Berger <i>et al.</i> (1991); Haddon (1995)
Ayers Rock	05/28/1989	Australian Craton (central & east), Australia	$m_b$ 5.8	Bowman <i>et al.</i> (1990)
Ungava	12/25/1989	Ungava Peninsula, Canada	$M_S$ 6.3	Bent (1994)
Sudan	05/20/1990	East African Rift System, Sudan	$M_S$ 7.2	Gaulon <i>et al.</i> (1992); Giardini and Beranzoli (1992); Girdler and McConnell (1994)
Sudan	05/24/1990	East African Rift System, Sudan	$M_S$ 6.4, 7.0	Gaulon <i>et al.</i> (1992); Giardini and Beranzoli (1992); Girdler and McConnell (1994)
Sudan	07/09/1990	East African Rift System, Sudan	$M_S$ 6.4	Gaulon <i>et al.</i> (1992); Giardini and Beranzoli (1992); Girdler and McConnell (1994)
Sudan	07/28/1990	East African Rift System, Sudan	$M_S$ 5.1	Gaulon <i>et al.</i> (1992); Giardini and Beranzoli (1992); Girdler and McConnell (1994)
Sudan	09/07/1990	East African Rift System, Sudan	$M_S$ 5.3	Gaulon <i>et al.</i> (1992); Giardini and Beranzoli (1992); Girdler and McConnell (1994)
Latur	09/30/1993	Latur, India	$M_w$ 6.3	Rajendran <i>et al.</i> (1996); Kayal <i>et al.</i> (1996)
Jabalpur	05/22/1997	Narmada Rift Basin, India	$m_b$ 6.0	Kayal (2000)
Bhuj	01/26/2001	Kachchh Rift Basin, India	$M_w$ 7.5	USGS-NEIC (2001); Kayal <i>et al.</i> (2002)

tonic stresses can cause a localized build-up of stresses and, ultimately, earthquakes. We then examined if these earthquakes occurred in the presence or absence of any of these stress concentrators. According to the global database of stable continental region earthquakes (Johnston *et al.*, 1994), “the strongest correlation of the entire data set of Stable Continental Region earthquakes (all magnitudes) is 64% for the category *extension or basin/graben*.” This implies that 64% of the global stable continental region seismicity is associated with extensional basins and/or grabens. Thus failed rifts form a major pre-existing zone of weakness for intraplate seismicity. When comparing the geological, geophysical, and seismological data, we therefore divided the examined intraplate earthquakes into those that were and were not associated with rifts (Tables 2 and 3). In both these tables only the larger earthquakes in any intraplate region have been listed.

### Examination of Data from Rift-associated Intraplate Locations

Table 2 lists twelve examples where the intraplate seismicity occurred within failed rifts ranging in age from Proterozoic to Cenozoic. According to Hasegawa (1991), most of the Charlevoix seismic zone in eastern Canada lies within a Proterozoic rift basin. However, Kumarapeli (1993) inferred it to be within the passive margin of the Iapetus ocean. We prefer the former classification and use it throughout the paper. The New Madrid seismic zone in the central U.S. and Saguenay graben in Canada lie within Paleozoic rifts (Van Arsdale *et al.*, 1998; Du Berger *et al.*, 1991). The North China rift basin and the Basel region in the Upper Rhine graben lie within rifts of Cenozoic age (Nabelek *et al.*, 1987; Shedlock *et al.*, 1987; Mayer *et al.*, 1997; Meghraoui *et al.*, 2001). The Middleton Place Summerville seismic zone near Charleston, South Carolina; Kachchh, India; and Swabian Jura in southwest Germany lie within Late Triassic–Early Jurassic rifts (Biswas, 1982; Illies, 1982; McBride *et al.*, 1989). The Godavari rift basin is Mesozoic in age (Chung, 1993), whereas the Narmada region lies within an Early Proterozoic rift basin (Valdiya, 1973). An Ordovician–Permian rift basin is host to the Amazonas (Nunn and Aires, 1988), while the Sudan seismic region lies within a rift of Cretaceous age (Girdler and McConnell, 1994). Thus the common factor in all of these locations of seismicity is the presence of a pre-existing zone of weakness—the rift—rather than its age.

The largest earthquakes in these twelve examples range from M 5.5 to M 8.1, and seven of them occur within the top 15 km of the crust (Table 2). The five exceptions are the Amazonas rift basin, where two large earthquakes occurred at depths of about 23 km and 45 km (Assumpção and Suarez, 1988; Zoback and Richardson, 1996), the Saguenay earthquake near the Saguenay graben (depth ~29 km) (Du Berger *et al.*, 1991; Haddon, 1995), the Bhuj earthquake in the Kachchh rift basin (depth ~17 km) (USGS-NEIC, 2001; Kayal *et al.*, 2002), and the Jabalpur earthquake in the Narmada rift basin (depth 36 km) (Kayal, 2000). Although the Saguenay earthquake occurred about 17 km south of the



▲ **Figure 1.** Saguenay graben seismogenic elements. The open box represents the region of granitic plutons and Charnockite-Mangerite intrusive site and cross-cutting discontinuous short lineaments. Modified from Hasegawa (1991).

Saguenay graben (Figure 1), based on the classification of Dewey (1988) of “basin exterior” earthquakes, Hasegawa (1991) suggested a possible causal association with the graben.

We also examined the style of faulting for each rift-associated intraplate location (Table 2) (Talwani and Rajendran, 1991; Zoback, 1992; Girdler and McConnell, 1994; Zoback and Richardson, 1996; Kayal, 2000; Meghraoui *et al.*, 2001; Kayal *et al.*, 2002). In eleven of the twelve examined rift-associated intraplate regions the main style of faulting is strike-slip, reverse, or a combination of both, indicating that the regions lie in compressional stress regimes. Normal faulting was observed at two locations. In the Basel region the normal faulting has been inferred based on paleoseismological and geomorphological data (Meghraoui *et al.*, 2001), but in the absence of seismological data this interpretation is poorly constrained. The mainshock of the Sudan earthquake sequence had left lateral strike-slip movement and some normal faulting. Both of these offsets appear to be due to associated kinematic adjustment in an overall compressive stress regime. Thus most cases of rift-associated intraplate regions lie in compressional regimes, as was also revealed from a global compilation of present-day tectonic stress patterns by Zoback *et al.* (1989). A notable exception is the Cenozoic Baikal rift system, where moderate seismicity is confined to middle and lower crustal depths and focal mechanisms indicate that the regional stress field is extensional in nature (Deverchere *et al.*, 1993; Deverchere *et al.*, 2001; Ten Brink and Taylor, 2002).

**TABLE 2**  
**Summary of Available Geological, Geophysical, and Seismological Data at Examined Rift-associated Intraplate Regions**

Stress Concentrators																
Location	Date	$M_{max}$	Focal Depth	Associated Rift	Age of Rift	Style of Faulting	Angle b/wn $S_{Hmax}$ and Major Fault	Intersecting Faults		Buried Plutons			Rift Pillow			
								(Y/N)	Length, Orientation (Fault 1)	Length, Orientation (Fault 2)	(Y/N)	Depth	Eq. Loc. wrt Pluton	Geol. of Pluton	(Y/N)	Z (km)
NMSZ, USA	12/16/1811	8.1	< 15 km!	Reelfoot Rift	Paleozoic	Strike-slip, Thrust	40°	Y	55 km, NE-SW	32 km, NW-SE (Fault 3: 30 km, NE-SW)	Y	2-10 km	Periphery	Mafic, Carbonatites	Proposed in Theoretical Model	30-32
MPSSZ, Charleston, USA	8/31/1886	7.3	< 12 km!	South Georgia Rift	Triassic-Jurassic	Strike-slip, Thrust	47°	Y	~200 km (~30 km is active), NNE	10-12 km, NW	Y	~1-4 km	Periphery	High Density (Basalt)	N	N/A
Godavari Rift Basin, India	4/13/1969	5.7	< 10 km!	Godavari Rift	Mesozoic	Strike-slip, Thrust	56°	Y	Not Known, NW-SE	Not Known, Nearly E-W	Not Evident	Within Upper Crust	Neighborhood of Intrusion	Basic in West and Northeast, Khondalites in Southeast	N	N/A
Narmada Rift Basin, India	1927, 5/22/1997	6.5*, 6.0*	~32-36 km	Narmada Rift	Early Proterozoic	Thrust	N/A	Y	~600 km, -E-W	Not Known, NW-SE	Y	Middle Crust	Neighborhood of Intrusions	High Density (Basalt)	Y	Between 20-30 km
Kachchh Rift Basin, India	1819, 2001	7.8, 7.6	~17 km	Kachchh Rift	Late Triassic-Early Jurassic	Strike-slip, Thrust	82°	Y	~200 km, -E-W	Not Known, NNE-SSW	Y	Within Upper Crust	Neighborhood of Intrusions	Deccan Basalts	N	N/A
Swabian Jura, Southwest Germany	11/16/1911	6.1	~10 km	Hohenzollern, Graben	Upper Jurassic-Miocene	Strike-slip	61°	Y	Not Known, N-S	Not Known, NE-SW	N	N/A	N/A	N/A	N	N/A
Amazonas Rift Basin, Brazil	8/5/1983	5.5*	45 km	Amazonas Rift	Ordovician-Permian	Thrust	N/A	N	N/A	N/A	Y	~15 km	Scattered around Intrusions	Ultrabasic	Y	~20
North China Rift Basin, China	7/27/1976	7.8**	~10 km	North China Rift	Middle Miocene-Cenozoic	Strike-slip, Thrust	36°	Y	Not Known, NE-SW	Not Known, NW-SE	N	N/A	N/A	N/A	N	N/A
St. Lawrence Rift, Canada	2/05/1663	7.0	~10 km!	St. Lawrence Rift	Proterozoic	Thrust	N/A	N	N/A	N/A	N	N/A	N/A	N/A	N	N/A
Upper Rhine Graben, Switzerland	10/18/1356	~6.0-6.5	~15 km!	Upper Rhine Graben	Cenozoic	Normal	N/A	Not Known	~10-15 km, NNE-SSW	N/A	Not Known	N/A	N/A	N/A	N	N/A
Saguenay Graben, Canada	11/25/1988	5.9*	~29 km	Saguenay Graben	Paleozoic	Thrust	N/A	Not Pronounced (many crosscutting lineaments)	~10 km; 0, 15, 30, 50, 105, and 160 degrees	N/A	Y	Middle-lower Crust	Scattered around Intrusions	Granite, Mangerite, Mafic Dikes, Gabbro	N	N/A
East African Rift System, Sudan	5/20/1990	7.2**	13 km	East African Rift	Cretaceous	Strike-slip, Normal	45°	Y	Few Hundred kms, -N-S	~150-200 km active zone, -NW-SE	Not Known	N/A	N/A	N/A	N	N/A

$M_{max}$ : maximum moment magnitude of an earthquake in the region; \*:  $m_b$ ; \*\*:  $M_s$ ; †: depth of network seismicity in general; Y: Yes; N: No.

**TABLE 3**  
**Summary of Available Geological, Geophysical, and Seismological Data at Examined Non-rift-associated Intraplate Regions**

Location	Date	$M_{max}$	Focal Depth	Intersecting Faults			Buried Plutons			Eq. Loc. wrt Pluton	Geol. of Pluton	Rift Pillow (Y/N)
				(Y/N)	Orientation (Fault 1)	Orientation (Fault 2)	(Y/N)	Depth				
Latur, India	9/30/1993	6.3*	~5 km	Y	NW-SE	NE-SW (Fault 3: E-W)	Y	3.5-12 km	Neighborhood of Intrusions	Granitic, Basic, High-density Metavolcanics	N	
Australian Craton (west), Australia	10/14/1968	6.8**	~3-7 km	N	N/A	N/A	Y	Not Known	Western Edge of Intrusions	Granite, Granite Gneiss	N	
Australian Craton (central & east), Australia	1/22/1988	6.7*	~3.5-6.5 km	N	N/A	N/A	Y	3.5-6.5 km in central craton; not known in eastern craton	Scattered around Intrusions	Granites, Sills and Dikes of Diorite and Lampropyre	N	
Illinois Basin, USA	9/27/1891	5.8*	<15 km!	Y	N-NE (WVFS, FAFC, CGL)	W-NW (TTZ, RCFS, CGFS)	Y	Within Upper Crust	Scattered around Intrusions	Igneous Compl., Mafic Dikes, Granite, Rhyolite, Plutonic & Volcanic Rocks, Some Basalt	N	
Ungava Peninsula, Canada	12/25/1989	6.3**	~3 km	N	-NE-SW	N/A	Not Known	N/A	N/A	N/A	N	
Guinea	12/22/1983	6.4	11 km	Y	NE (Trans-Am Frac. Zone)	WNW-ESE	Not Known	N/A	N/A	N/A	N	
Ghana	1939	6.5	~16 km	Y	NE (Akwapim Fault)	E-W (Coastal Bound. Fault)	Not Known	N/A	N/A	N/A	N	
Miramichi, Canada	1/09/1982	5.7	~7 km	Y	Conjugate Fault	Conjugate Fault	Y	~10 km	Scattered around Intrusion	Granitic	N	

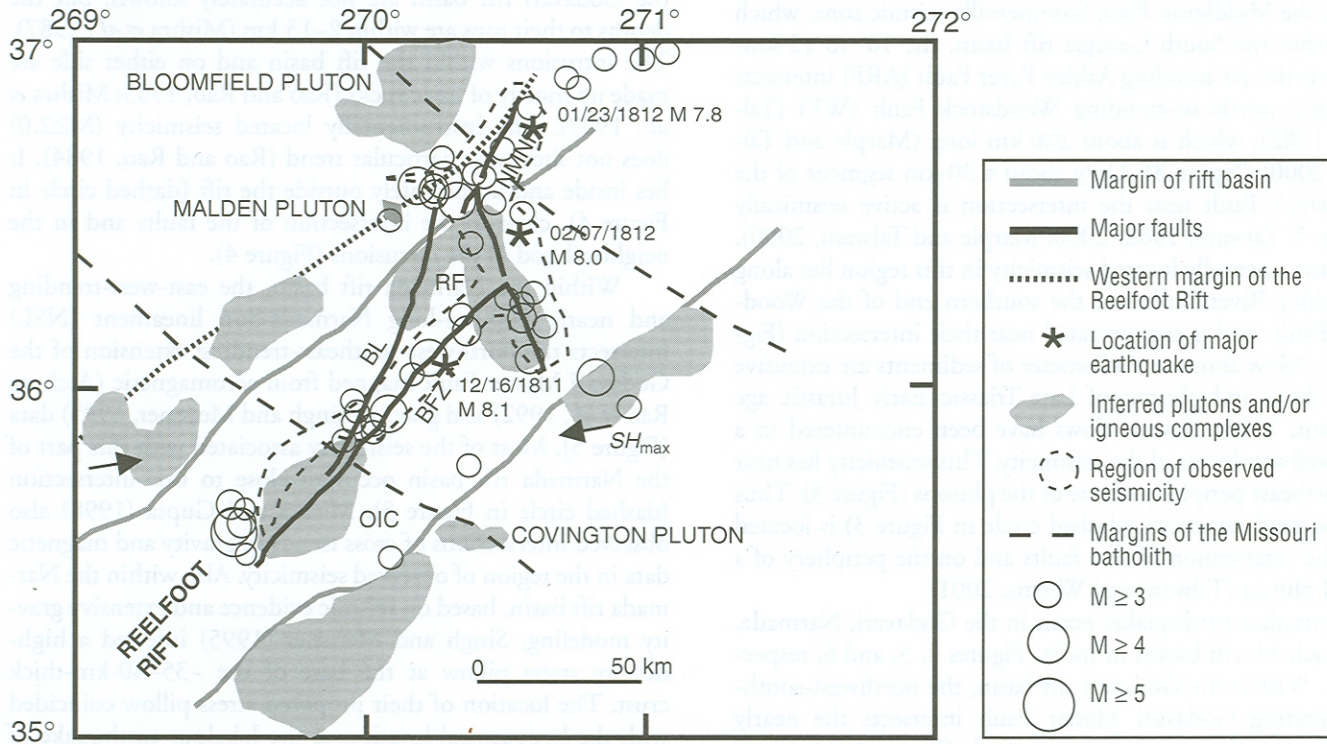
$M_{max}$ : maximum moment magnitude of an earthquake in the SCR region; \*:  $m_b$ ; \*\*:  $M_s$ ; !: depth of network seismicity in general; Y: Yes, N: No.

For each case study we identified the possible stress concentrator(s) listed in Table 2. This table also provides the orientation of the intersecting faults, depth of the buried pluton, location of earthquakes with respect to the buried pluton, and the depth to the top of the rift pillow.

We illustrate our approach to explain intraplate seismicity using the New Madrid seismic zone case study, because of the good data control. In Figure 2 we compare instrumentally located M 3.0 or greater earthquakes with geologically and geophysically outlined structures. In the New Madrid seismic zone, within the northeast-southwest-trending, nearly 400-km-long and 100-km-wide Reelfoot Rift, there are two intersecting fault zones, the 55-km-long Blytheville fault zone (BFZ), oriented northeast-southwest, and the 32-km-long Reelfoot Fault (RF), oriented northwest-southeast (Figure 2; Van Arsdale *et al.*, 1995; Johnston and Schweig, 1996). A third fault, the New Madrid North Fault (NMNF), lies outside the edge of the floor of the Reelfoot Rift but within its shallower edge (Figure 2; Rhea and Wheeler, 1995). This ~30-km-long north-northeast-trending fault is considered to be the extension of the aseismic Bootheel lineament (BL) by Johnston and Schweig (1996). Wheeler (2003) and Hough (2003) (personal communications) questioned this connection, however. The Missouri batholith, a prominent, 100-km-wide, low-density, granitic, upper-crustal structure, trends northwest-southeast and crosscuts the Reelfoot Rift

(Figure 2; Hildenbrand *et al.*, 1996; Hildenbrand *et al.*, 2001). The observed seismicity inside the Reelfoot Rift is located along the Blytheville fault zone and the Reelfoot and New Madrid North Faults (Figure 2). In particular there is clustering of the larger earthquakes near the intersections of the Bootheel lineament and Blytheville fault zone; Reelfoot Fault and Blytheville fault zone; and Reelfoot Fault and New Madrid North Fault (Figure 2). A few earthquakes are also located along the southern margin of the rift (Figure 2).

The major plutons in the New Madrid seismic zone (Figure 2) are at a depth of about 2–10 km (Hildenbrand *et al.*, 2001). They are mostly mafic in nature. The large intrusions along the Reelfoot Rift margins were inferred by Hildenbrand and Hendricks (1995) to range in age from early Paleozoic to Cretaceous. The major intrusions in the New Madrid seismic zone are the Bloomfield and Covington plutons and Osceola Igneous Complex (OIC). Based on available drillhole data very close to these plutons, Hildenbrand *et al.* (2001) inferred the Bloomfield and Covington plutons to be of pre-Ordovician and Late Triassic–Middle Jurassic age respectively. The Osceola Igneous Complex was inferred to be Permian based on geochemical and petrological studies (Hildenbrand *et al.*, 2001). We note that there is seismicity at or near the northern and southern ends of OIC, and the northwestern and southeastern edges of the unnamed pluton near Reelfoot Fault (Figure 2). The large cluster of seismicity



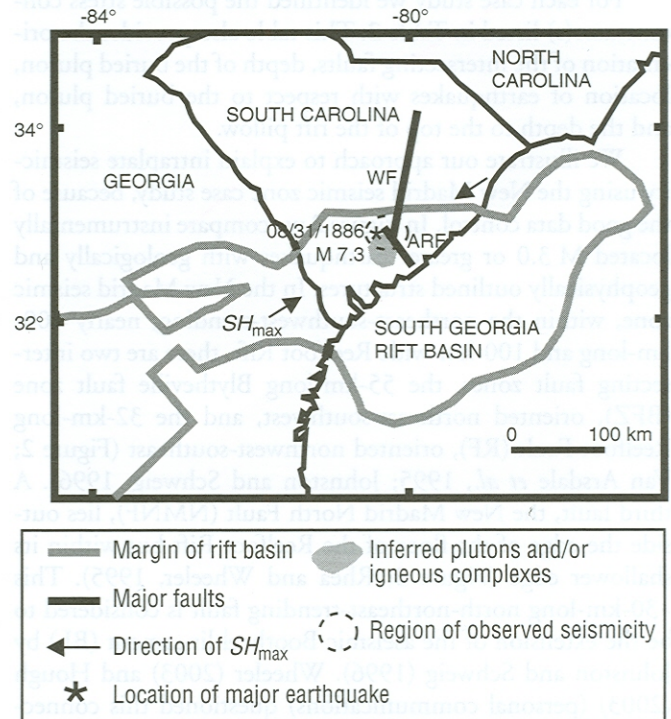
▲ **Figure 2.** Map showing New Madrid seismic zone and seismogenic elements. The margins of the Reelfoot Rift floor, outlines of plutons and igneous complexes, faults, and margins of the Missouri batholith have been taken from Hildenbrand *et al.* (2001). The edge of the western margin of the Reelfoot Rift has been adopted from Rhea and Wheeler (1995). BFZ: Blytheville Fault Zone; RF: Reelfoot Fault; NMNF: New Madrid North Fault; BL: Bootheel lineament; OIC: Osceola Igneous Complex. Open circles represent instrumentally located seismicity of M  $\geq$  3.0 from 1974–2002 from CERL, Memphis catalog.

lying near the intersection of the New Madrid North Fault, Bootheel lineament, and Reelfoot Fault is also between the Bloomfield pluton to the north and an unnamed pluton complex to the south. Interestingly, most of the seismicity forms a halo around the pluton and does not lie in the pluton itself, as was observed by Ravat *et al.* (1987). A possible exception is the southern leg of the Reelfoot Fault. We also note that three of the four earthquakes that occurred near the southern margin of the rift were located on the periphery of plutons outside the rift basin. Thus the spatial association of seismicity with the location of fault intersections and the periphery of plutons possibly suggest a causal association.

Next we examined similar site-specific geological, geophysical, and seismological data for other locations of seismicity. The data related to seismogenesis at these locations are not as uniform or as detailed as those available for the New Madrid seismic zone. To compare the data at other locations of intraplate seismicity, we present these data schematically showing the faults, mainshock, outline of the areas of seismicity, and plutons using the same symbols. A lower crustal rift pillow has been theoretically modeled in the New Madrid seismic zone at a depth of 30–32 km (Stuart *et al.*, 1997). The modeled depth is greater than the observed seismicity, however, which makes its presence questionable as a stress concentrator. Therefore it has not been included in Figure 2. As is noted in Figure 2, seismicity is located near the intersections of the faults and on the periphery of the buried plutons.

In the Middleton Place Summerville seismic zone, which lies within the South Georgia rift basin, the 10- to 12-km-long, northwest-trending Ashley River Fault (ARF) intersects the north-northeast-trending Woodstock Fault (WF) (Talwani, 1982), which is about 200 km long (Marple and Talwani, 2000) (Figure 3). Only about a 30-km segment of the Woodstock Fault near the intersection is active seismically (Figure 3; Talwani, 1982, 2000; Marple and Talwani, 2000). The instrumentally located seismicity in this region lies along the Ashley River Fault and the southern end of the Woodstock Fault, and is concentrated near their intersection (Figure 3). Below about one kilometer of sediments are extensive basalt flows and plutons of Late Triassic–Early Jurassic age (Talwani, 1985). Several flows have been encountered in a deep well southwest of the seismicity. This seismicity lies near the northeast periphery of one of the plutons (Figure 3). Thus the observed seismicity (dashed circle in Figure 3) is located near the intersection of two faults and on the periphery of a buried pluton (Talwani and Weems, 2001).

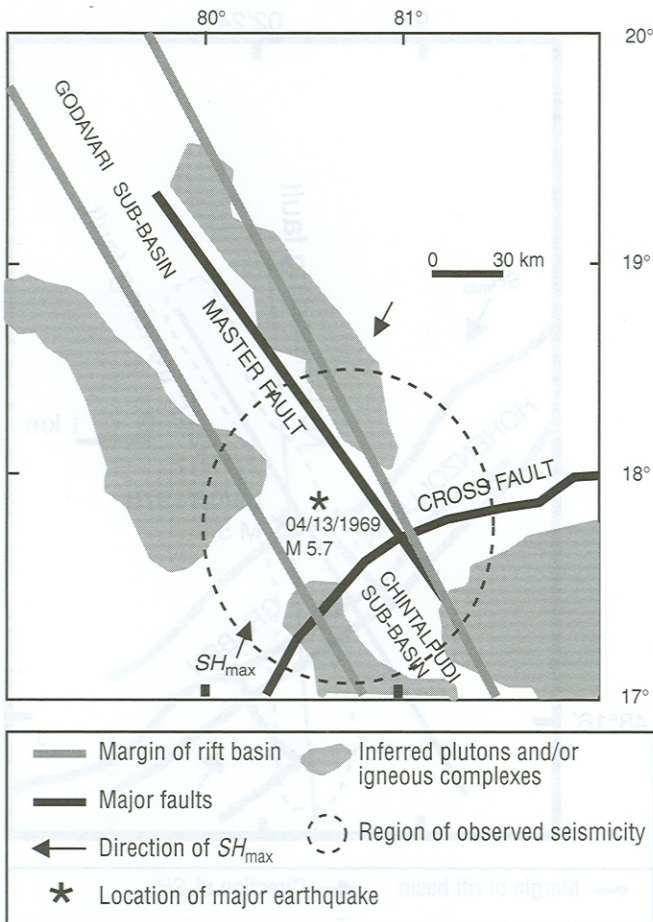
Intraplate earthquakes occur in the Godavari, Narmada, and Kachchh rift basins in India (Figures 4, 5, and 6, respectively). Within the Godavari rift basin, the northwest-southeast-trending Godavari Master Fault intersects the nearly east-west-trending Godavari cross-fault (Figure 4; Mishra *et al.*, 1987). The mainshock on 13 April 1969, the M 5.7 Bhadrachalam earthquake, located using WWSSN data, with a focal mechanism indicating northwest-southeast and northeast-southwest nodal planes, occurred about 30 km from this intersection (Figure 4). The outlines of the intrusive bodies in



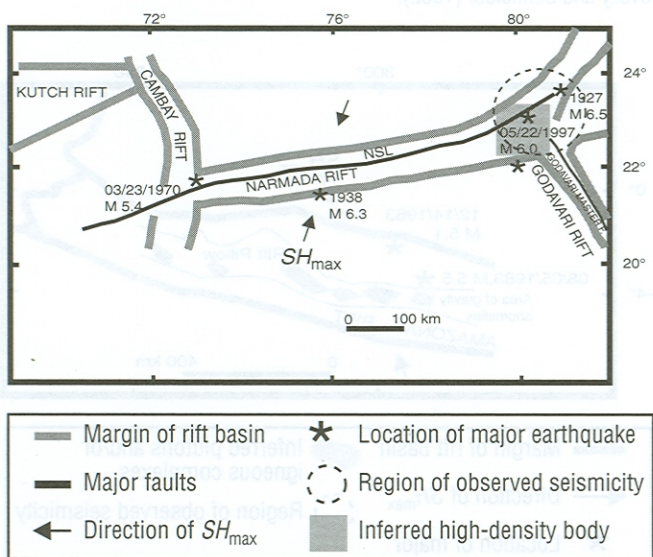
▲ **Figure 3.** Middleton Place-Summerville seismic zone seismogenic elements. Rift margin from McBride *et al.* (1989).

the Godavari rift basin are not accurately known, but the depths to their tops are within 2–13 km (Mishra *et al.*, 1987). The intrusions within the rift basin and on either side are made up mostly of basic rocks (Rao and Rao, 1983; Mishra *et al.*, 1987). The instrumentally located seismicity ( $M \geq 2.0$ ) does not show any particular trend (Rao and Rao, 1984). It lies inside and immediately outside the rift (dashed circle in Figure 4), close to the intersection of the faults and in the neighborhood of the intrusions (Figure 4).

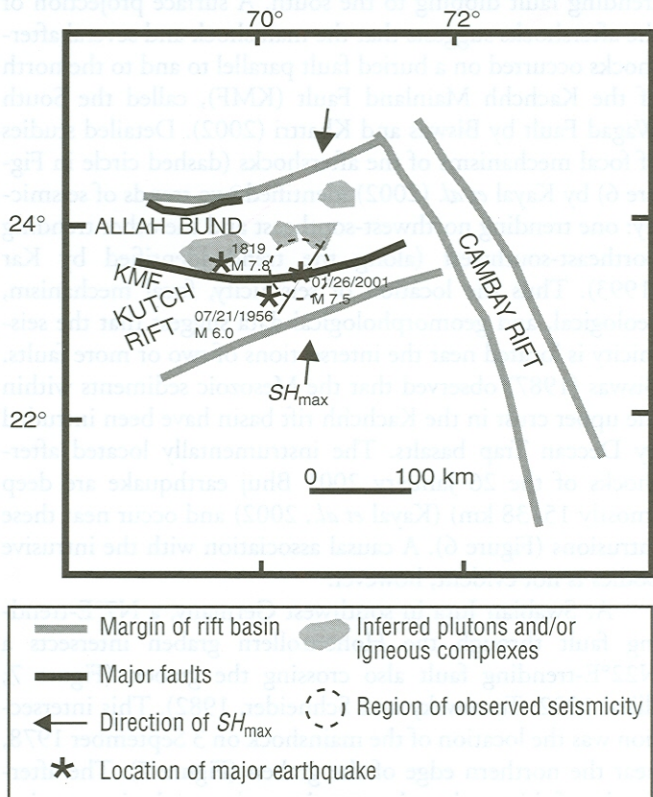
Within the Narmada rift basin, the east-west-trending and nearly 600-km-long Narmada-Son lineament (NSL) intersects the northwest-southeast-trending extension of the Godavari Master Fault mapped from aeromagnetic (Atchuta Rao *et al.*, 1992) and gravity (Singh and Meissner, 1995) data (Figure 5). Most of the seismicity associated with this part of the Narmada rift basin occurred close to this intersection (dashed circle in Figure 5). Mishra and Gupta (1998) also observed intersections of cross trends in gravity and magnetic data in the region of observed seismicity. Also within the Narmada rift basin, based on seismic evidence and extensive gravity modeling, Singh and Meissner (1995) inferred a high-density stress pillow at the base of the ~35–40-km-thick crust. The location of their proposed stress pillow coincided with the hypocentral location of the Jabalpur earthquake of 22 May 1997. Later, a similar high-density body in the same region, the top of which was at midcrustal depths, was also inferred based on gravity and magnetic data (Figure 5; Mishra and Gupta, 1998; Mishra and Ravi Kumar, 1998). Rajendran and Rajendran (1998) suggested a causal relationship



▲ **Figure 4.** Godavari seismogenic elements. Modified from Mishra *et al.* (1987).



▲ **Figure 5.** Narmada seismogenic elements. Modified from Singh and Meissner (1995).



▲ **Figure 6.** Kachchh seismogenic elements. Modified from Biswas (1982).

between this rift pillow located in the hypocentral depth range (20–36 km) and the 22 May 1997 Jabalpur earthquake. Furthermore, analysis of seismic refraction data by Kumar *et al.* (2000) indicated an anomalously high-velocity layer with varying thicknesses, which was interpreted to be the top of this rift pillow at midcrustal depths. Thus these observations suggest a causal relationship of the rift pillow with the seismicity in the Narmada rift basin.

Two other notable earthquakes in the Narmada rift basin are the 23 March 1970  $M_w$  5.4 Broach earthquake and the 1938  $m_b$  6.3 Satpura earthquake (Figure 5). The Broach earthquake was located in the Cambay graben near its intersection with the Narmada rift basin. The fault-plane solution for this earthquake shows a nearly east-west-trending nodal plane, suggesting a possible association with the Narmada-Son lineament (Chung, 1993). The historical Satpura earthquake, on the other hand, whose focal depth was reported to be ~40 km based on instrumentally recorded data (Rajendran and Rajendran, 1998), is considered to be associated with the Tapti lineament, which coincides with the southern edge of the Narmada rift basin (Figure 5).

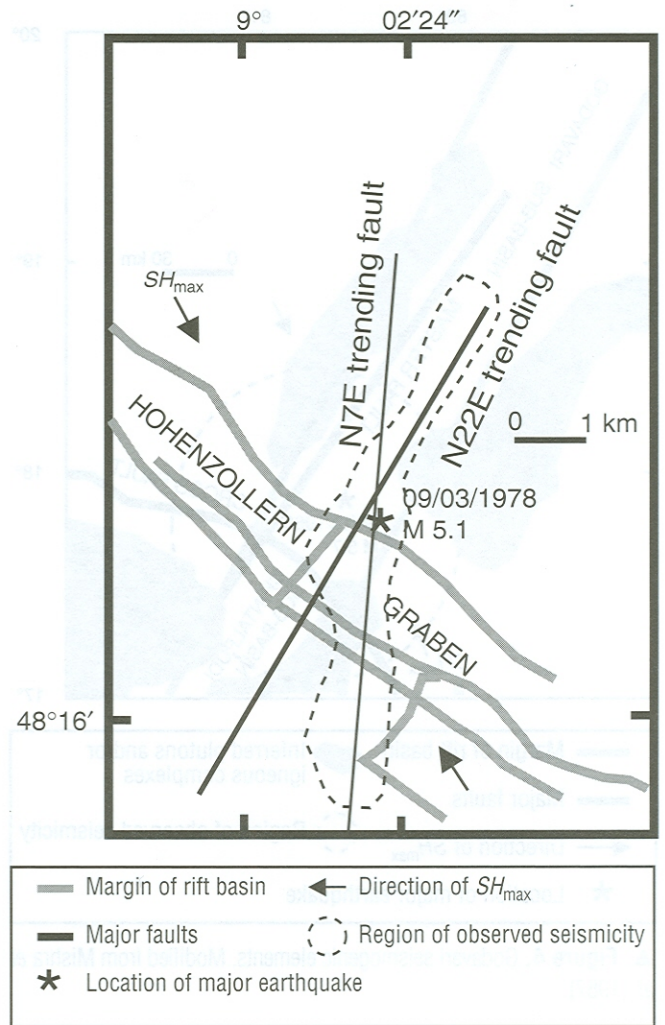
In the Kachchh rift basin various east-west-trending faults are offset in a right-lateral sense by a northeast-trending feature first identified by Kar (1993) based on geomorphological and satellite data (Talwani and Gangopadhyay, 2001). The focal mechanism and the location of the mainshock on 26 January 2001 suggest that it occurred on an east-west-

trending fault dipping to the south. A surface projection of the aftershocks suggests that the mainshock and several aftershocks occurred on a buried fault parallel to and to the north of the Kachchh Mainland Fault (KMF), called the South Wagad Fault by Biswas and Khattri (2002). Detailed studies of focal mechanisms of the aftershocks (dashed circle in Figure 6) by Kayal *et al.* (2002) identified two trends of seismicity: one trending northwest-southeast and the other trending northeast-southwest (along the trend identified by Kar (1993)). Thus the location of seismicity, focal mechanism, geological, and geomorphological data suggest that the seismicity is located near the intersections of two or more faults. Biswas (1987) observed that the Mesozoic sediments within the upper crust in the Kachchh rift basin have been intruded by Deccan Trap basalts. The instrumentally located aftershocks of the 26 January 2001 Bhuj earthquake are deep (mostly 15–38 km) (Kayal *et al.*, 2002) and occur near these intrusions (Figure 6). A causal association with the intrusive bodies is not evident, however.

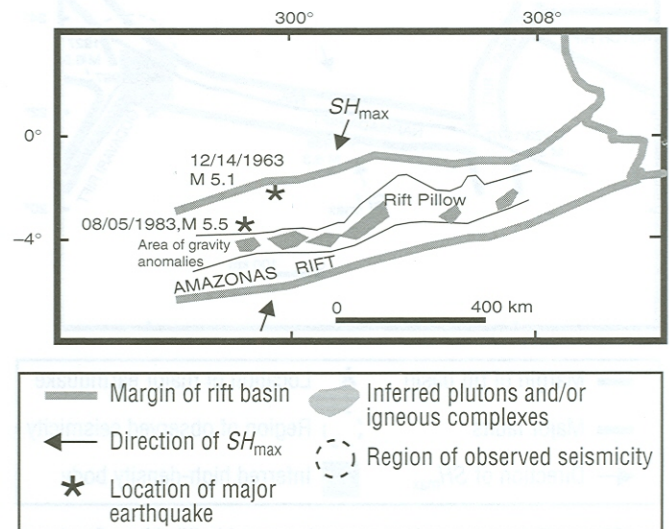
At Swabian Jura in southwest Germany, a N7°E-trending fault through the Hohenzollern graben intersects a N22°E-trending fault also crossing the graben (Figure 7; Illies, 1982; Turnovsky and Schneider, 1982). This intersection was the location of the mainshock on 3 September 1978, near the northern edge of the graben (Figure 7). The aftershocks of this earthquake were located near the intersection of these two faults within the graben and also along the northern leg of the N22°E-trending fault and the southern leg of the N7°E-trending fault immediately outside the graben (dashed area in Figure 7). Two other major earthquakes of M 5.2 and M 6.1 also occurred in the Swabian Jura region (Table 1), but accurate instrumental locations are not available.

In the Amazonas rift basin, Nunn and Aires (1988) have outlined ultrabasic intrusive bodies at a depth of about 15 km based on a chain of nearly east-west-trending Bouguer gravity highs. A high-density rift pillow varying from 100–200 km in width and 22–25 km in thickness has been postulated in the lower crust inside the rift basin (Zoback and Richardson, 1996). The seismicity that occurred near the northern margin of the rift basin and for which focal mechanisms are available suggests approximately east-west-trending nodal planes at depths of 23 km and 45 km respectively (Figure 8; Zoback and Richardson, 1996). This seismicity has been causally associated with the rift pillow based on the modeling by Zoback and Richardson (1996) and because of its spatial association as described above.

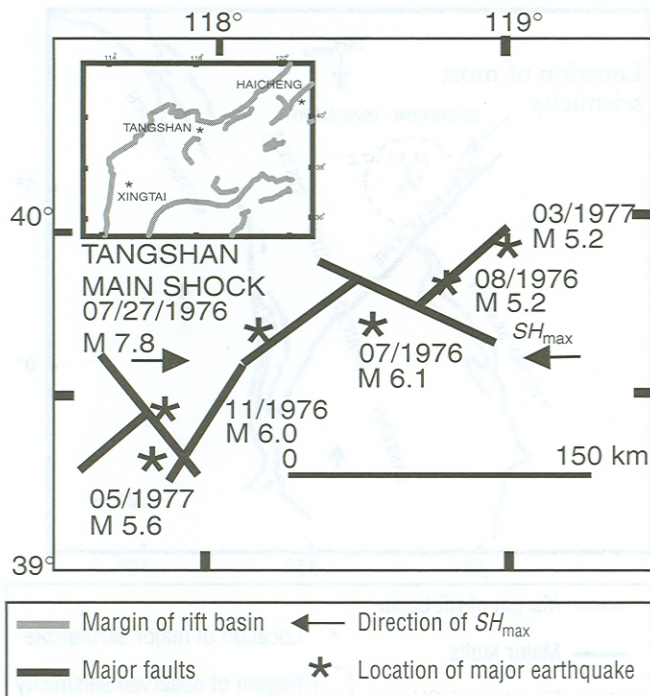
The North China rift basin has been the host of several large intraplate earthquakes in the last four decades, particularly the 6 March 1966  $M_w$  7.3 Xingtai, 4 February 1975  $M_w$  7.3 Haicheng, and 27 July 1976  $M_s$  7.8 Tangshan earthquakes (Figure 9 inset). The Tangshan earthquake sequence (Figure 9) was the most destructive of these events (Nabelek *et al.*, 1987). In the Tangshan region within the North China rift basin, several faults oriented northeast, northwest, and west-northwest intersect in an en-echelon pattern (Figure 9;



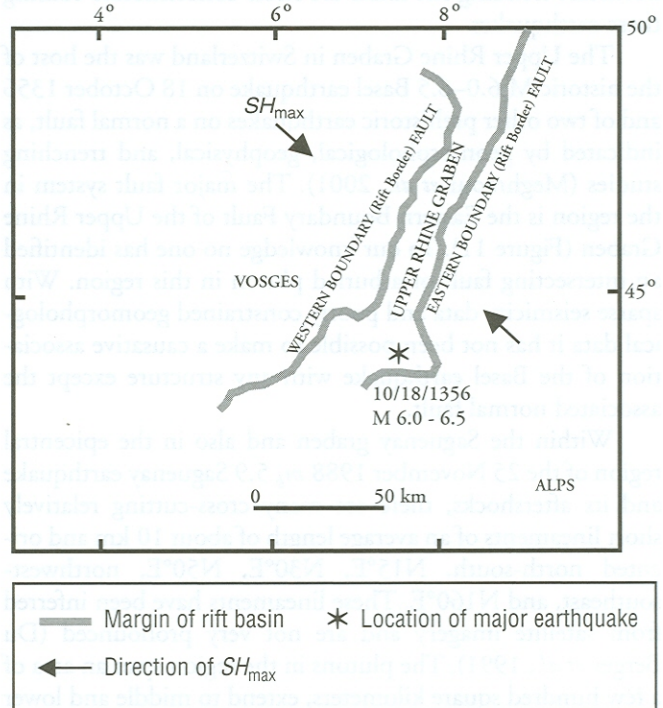
▲ Figure 7. Swabian Jura seismogenic elements. Modified from Turnovsky and Schneider (1982).



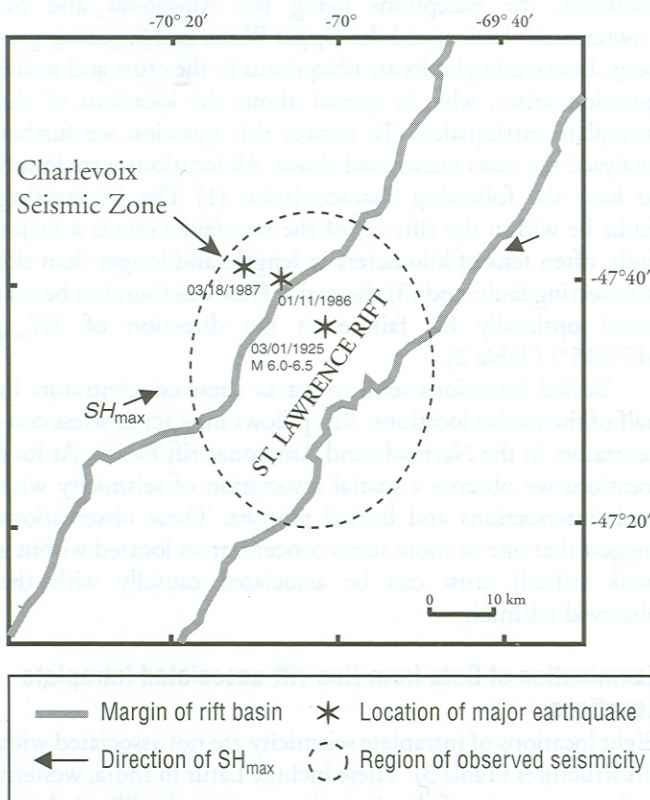
▲ Figure 8. Amazonas seismogenic elements. Modified from Nunn and Aires (1988).



▲ **Figure 9.** North China Rift basin seismogenic elements. Modified from Shedlock *et al.* (1987).



▲ **Figure 11.** Upper Rhine graben seismogenic elements. (Modified from Meghraoui *et al.* (2001).



▲ **Figure 10.** St. Lawrence Rift seismogenic elements. Modified from Hasegawa (1991).

Shedlock *et al.*, 1987). The Tangshan mainshock occurred on a northeast-trending right-lateral strike-slip fault (Figure 9; Shedlock *et al.*, 1987). The foreshocks and aftershocks define two northwest-trending zones separated by a northeast-southwest-trending fault (Shedlock *et al.*, 1987). Thus we note that in the North China rift basin the epicentral locations of the major earthquakes correlate well with the fault intersections, suggesting a causal association with the intersections (Figure 9).

Two of the rift-associated intraplate locations examined in this paper do not show conclusive evidence of the presence of any stress concentrators. These are the Charlevoix seismic zone (Figure 10) and Upper Rhine Graben in Switzerland (Figure 11). The Charlevoix seismic zone in the St. Lawrence Rift has been host to several major earthquakes in southeast Canada, such as the 5 February 1663 M  $7.0 \pm 0.5$  earthquake and its larger aftershocks (epicenters usually assigned to the Charlevoix seismic zone; Ebel, 1996) and the 1 March 1925 M 6.0–6.5 earthquake (Figure 10; Bent, 1992). The instrumentally located seismicity in the Charlevoix seismic zone, most of which lies within the St. Lawrence Rift (dashed ellipse in Figure 10), is postulated to be due to activation of northeast-striking ancient rift faults that were probably weakened by a Paleozoic meteor impact (Hasegawa, 1991; Bent, 1992). Two of the larger earthquakes in the region between 1988 and 1995 (Figure 10) occurred on west-northwest–east-southeast–trending lineaments reactivated by the meteor impact (Lamontagne, 1997). However, it is not clear whether the intersection of these lineaments with the dominant

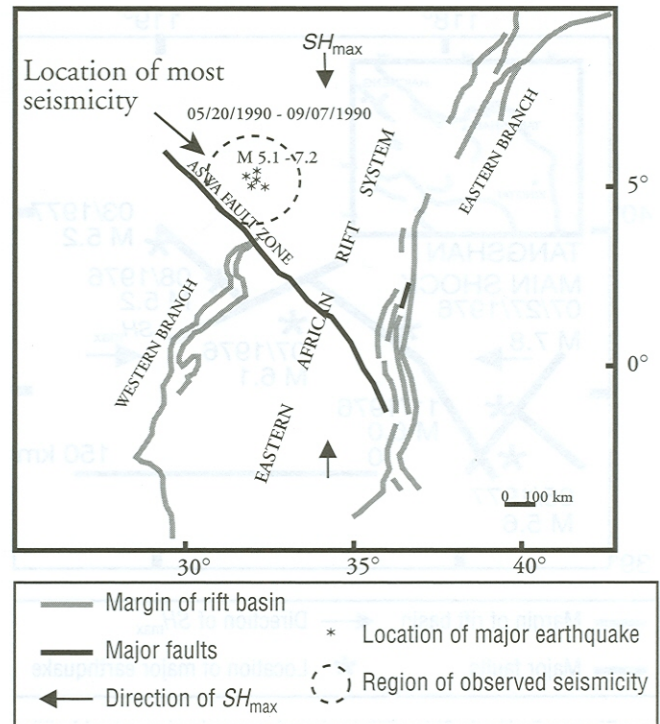
northeast-trending rift faults are stress concentrators causing these earthquakes.

The Upper Rhine Graben in Switzerland was the host of the historic M 6.0–6.5 Basel earthquake on 18 October 1356 and of two other prehistoric earthquakes on a normal fault, as indicated by geomorphological, geophysical, and trenching studies (Meghraoui *et al.*, 2001). The major fault system in the region is the Eastern Boundary Fault of the Upper Rhine Graben (Figure 11). To our knowledge no one has identified an intersecting fault or a buried pluton in this region. With sparse seismicity data and poorly constrained geomorphological data it has not been possible to make a causative association of the Basel earthquake with any structure except the associated normal fault.

Within the Saguenay graben and also in the epicentral region of the 25 November 1988  $m_b$  5.9 Saguenay earthquake and its aftershocks, there are many cross-cutting relatively short lineaments of an average length of about 10 km and oriented north-south, N15°E, N30°E, N50°E, northwest-southeast, and N160°E. These lineaments have been inferred from satellite imagery and are not very pronounced (Du Berger *et al.*, 1991). The plutons in the region span an area of a few hundred square kilometers, extend to middle and lower crustal depths, and are mostly composed of granite, mangerite, mafic dikes, and gabbro (Figure 1; Du Berger *et al.*, 1991; Hasegawa, 1991; Talwani and Rajendran, 1991). The 1988 Saguenay mainshock was located at a depth of 29 km and the aftershocks in the region (dashed circle in Figure 1) were at depths of 15–30 km (Du Berger *et al.*, 1991). The uncertainty about the plane of failure and the large depth of the earthquake preclude the inference of any causal association.

In the East African Rift system, the nearly north-south-trending rift border faults of the western and eastern branches of the rift system have been cross-cut by the northwest-southeast-trending Aswa fault zone (Figure 12; Gaulon *et al.*, 1992; Girdler and McConnell, 1994). Among the six major events of the Sudan earthquake sequence, two appeared to have focal mechanisms indicating their association with the northwest-southeast-trending Aswa fault zone and other similarly trending lineaments. The remaining four earthquakes have focal mechanisms indicating that they were associated with the north-northeast-trending rift border faults (Girdler and McConnell, 1994). Most of the seismicity is located near the intersection of the north-northeast-trending rift border faults and northwest-southeast-trending Aswa fault zone (dashed circle in Figure 12). Girdler and McConnell (1994) also observed that the mainshock of 20 May 1990 triggered activity on the north-northeast-trending rift border faults followed by seismicity alternating between the two intersecting fault systems oriented almost perpendicular to each other. This observation coupled with the spatial association of the seismicity with the intersections strongly suggests a causal association.

In summary, based on our analysis, of the twelve cases of rift-associated intraplate regions examined in this paper, intersecting faults appear to act as stress concentrators at eight



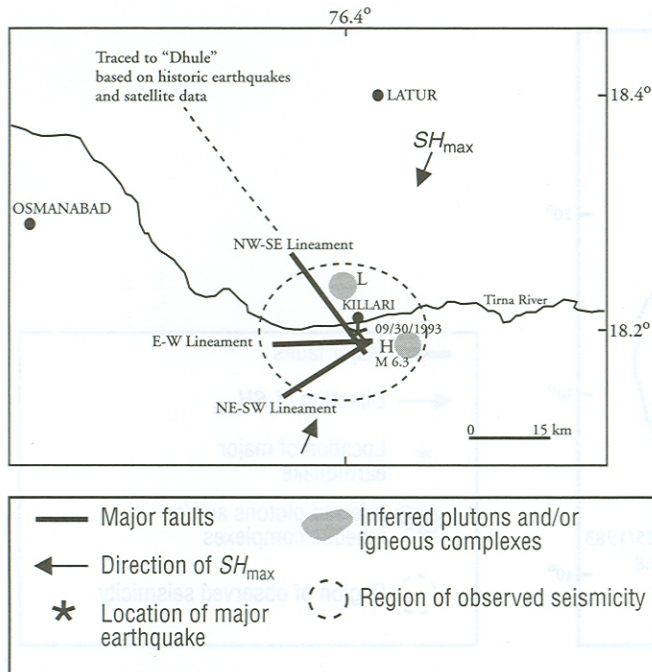
▲ **Figure 12.** East African Rift system seismicogenic elements. Modified from Gaulon *et al.* (1992).

locations, the exceptions being the Amazonas and St. Lawrence rift basins, and the Upper Rhine and Saguenay grabens. Intersecting faults are ubiquitous in the crust and so the question arises, what is special about the locations of the intraplate earthquakes? To answer this question we further analyzed the cases mentioned above. All locations were found to have the following characteristics: (1) The intersecting faults lie within the rift; (2) of the two faults one is a major fault, often tens of kilometers in length, and longer than the intersecting fault; and (3) the major fault was found to be oriented optimally for failure to the direction of  $SH_{max}$  ( $45^\circ \pm 15^\circ$ ) (Table 2).

Buried intrusions tend to act as stress concentrators in half of the twelve locations. Rift pillows may act as stress concentrators in the Narmada and Amazonas rift basins. At four locations we observe a spatial association of seismicity with both intersections and buried plutons. These observations suggest that one or more stress concentrators located within a weak (rifted) crust can be associated causally with the observed seismicity.

### Examination of Data from Non-rift-associated Intraplate Locations

Eight locations of intraplate seismicity are not associated with rift structures (Table 3). These include Latur in India, western and eastern parts of the Australian craton, the Illinois basin including the Wabash Valley in USA, Ungava Peninsula in Canada, Guinea, southeast Ghana, and Miramichi in Canada. Interestingly, all these regions lie within Precambrian



▲ **Figure 13.** Latur seismogenic elements. Modified from Kayal *et al.* (1996). Trace of NW-SE lineament from Rajendran *et al.* (1996). Solid gray circles show locations of gravity “lows” (L) and “highs” (H) from Mishra *et al.* (1998).

cratons. The largest earthquake in any of these regions ranges between M 5.7 and M 6.8 (Table 3). All the seismicity observed in these regions occurred within the upper crust and at five locations it occurred within the top 7 km.

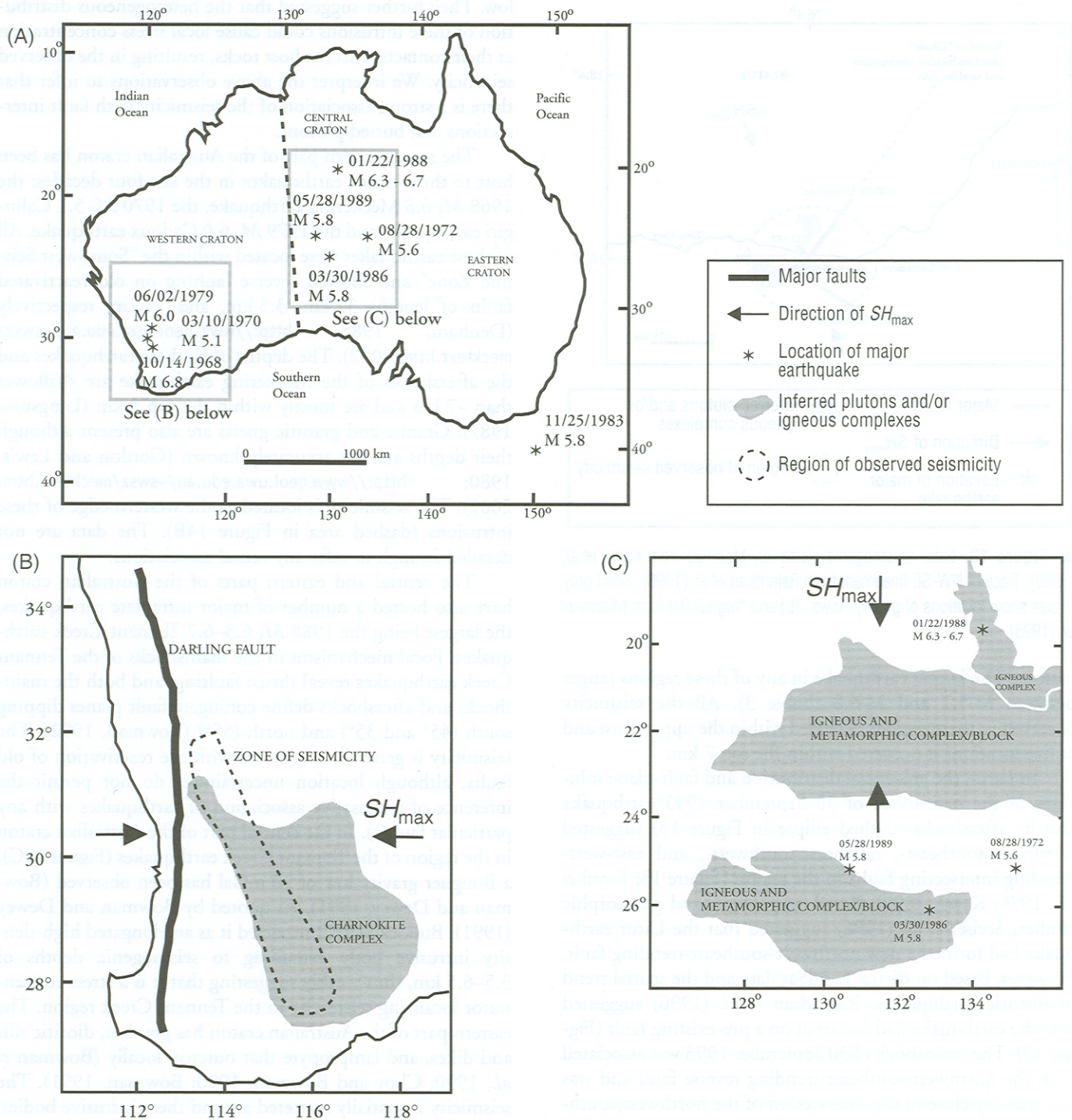
In Latur, the epicentral distribution and fault-plane solutions of the mainshock of 30 September 1993 earthquake and its aftershocks (dashed ellipse in Figure 13) suggested northwest-southeast-, northeast-southwest-, and east-west-trending intersecting faults in the region (Figure 13; Kayal *et al.*, 1996; Kayal, 2000). Based on geologic and geomorphic studies, Seeber *et al.* (1996) suggested that the Latur earthquake had formed a new northwest-southeast-trending fault. However, based on digital LandSat data and the spatial trend of historic earthquakes, Rajendran *et al.* (1996) suggested that the earthquake had occurred on a pre-existing fault (Figure 13). The mainshock of 30 September 1993 was associated with the northwest-southeast-trending reverse fault and was located very close to the intersection of the northwest-southeast and east-west-trending faults (Figure 13). Gravity modeling by Mishra *et al.* (1998) showed that elongated short wavelength lows delineate low-density rocks in the upper crust (tops at 10–12 km) warping up to a depth of 3.5 km. Elongated short wavelength highs were interpreted by them to be associated with granite and basic high density metavolcanic rocks (Figure 13). The focal depths of the mainshock and the aftershocks were also in the depth range of 3–12 km. Mishra *et al.* (1998) also noted that the epicenter of the mainshock lies between the gravity highs and lows and the epicenters of the aftershocks are mainly in the vicinity of the gravity

low. They further suggested that the heterogeneous distribution of these intrusions could cause local stress concentration at their contacts with the host rocks, resulting in the observed seismicity. We interpret the above observations to infer that there is a strong association of the seismicity with fault intersections and buried plutons.

The southwestern part of the Australian craton has been host to three major earthquakes in the last four decades: the 1968  $M_S$  6.8 Meckering earthquake, the 1970  $M_S$  5.1 Calingiri earthquake, and the 1979  $M_S$  6.0 Cadoux earthquake. All of these earthquakes were located within the “Southwest Seismic Zone” and showed reverse faulting on old reactivated faults of lengths 37 km, 3.5 km, and 15 km, respectively (Denham, 1988; <http://www.geol.uwa.edu.au/~swsz/mecktext.htm>, 2002). The depths of all these earthquakes and the aftershocks of the Meckering earthquake are shallower than ~7 km and are mostly within the top 3 km (Langston, 1987). Granite and granitic gneiss are also present although their depths are not accurately known (Gordon and Lewis, 1980; <http://www.geol.uwa.edu.au/~swsz/mecktext.htm>, 2002). The seismicity is located at the western edge of these intrusions (dashed area in Figure 14B). The data are not detailed enough to infer any causal associations.

The central and eastern parts of the Australian craton have also hosted a number of major intraplate earthquakes, the largest being the 1988  $M_S$  6.3–6.7 Tennant Creek earthquakes. Focal mechanisms of the mainshocks of the Tennant Creek earthquakes reveal thrust faulting, and both the mainshocks and aftershocks define conjugate fault planes dipping south ( $45^\circ$  and  $35^\circ$ ) and north ( $55^\circ$ ) (Bowman, 1992). The seismicity is generally associated with the reactivation of old faults, although location uncertainties do not permit the inference of a causative association of earthquakes with any particular fault(s). In the central part of the Australian craton in the region of the Tennant Creek earthquakes (Figure 14C), a Bouguer gravity low of 20 mGal has been observed (Bowman and Dewey, 1991). As quoted by Bowman and Dewey (1991), Bullock (1977) modeled it as an elongated high-density intrusive body extending to seismogenic depths of 3.5–6.5 km, thus weakly suggesting that it is a stress concentrator localizing seismicity in the Tennant Creek region. The eastern part of the Australian craton has granites, dioritic sills and dikes, and lamprophyre that outcrop locally (Bowman *et al.*, 1990; Choy and Bowman, 1990; Bowman, 1991). The seismicity is spatially scattered around these intrusive bodies, but lack of accurate hypocentral information and data pertaining to the depths of these intrusions inhibits any causal association with the seismicity.

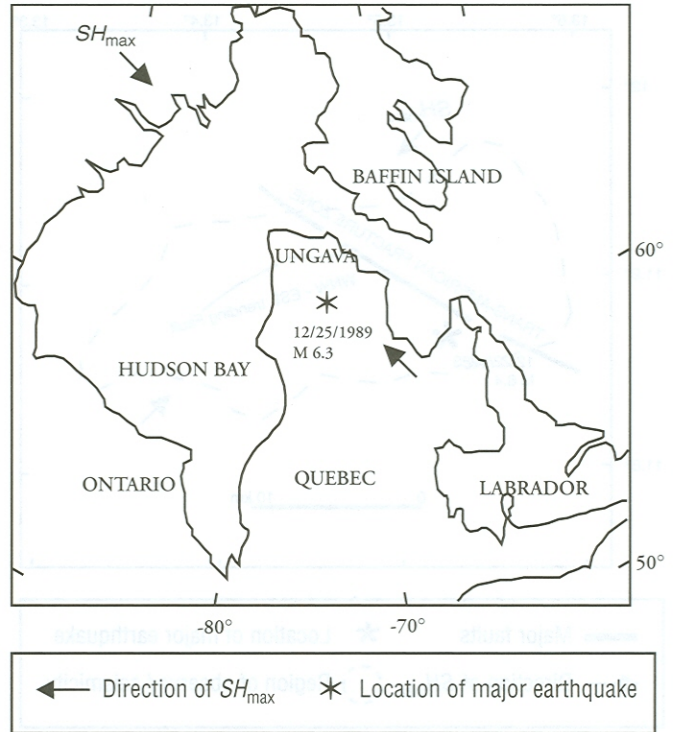
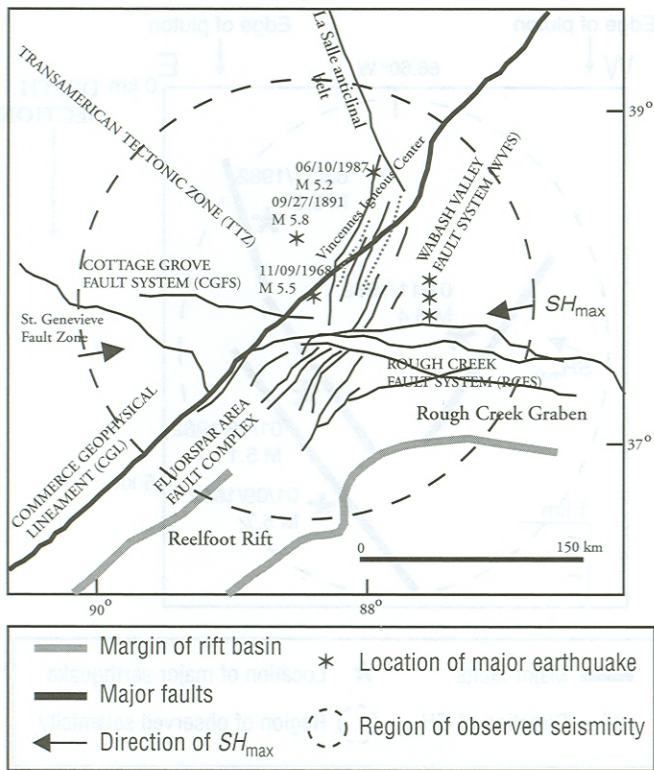
The Illinois basin, which includes the Wabash Valley, is to the north of the Reelfoot Rift, which encompasses the New Madrid seismic zone. The 50–200-km-long north-northeast-trending Wabash Valley fault system (WVFS) and Commerce geophysical lineament (CGL) lie almost orthogonally to the Cottage Grove fault system (CGFS), the La Salle anticlinal belt, and the >50 km west-northwest-trending Trans-American Tectonic Zone (TTZ), respectively (Figure



▲ **Figure 14.** Australian craton seismogenic elements. (A) Dotted line separates western from central and eastern parts of the craton; modified from Crone et al. (1992). (B) Western part of craton modified from <http://www.geol.uwa.edu.au/~swsz/swsz.htm#doyle> (2002). (C) Eastern part of craton modified from Bowman et al. (1990).

15; Kolata and Hildenbrand, 1997; Marshak and Paulsen, 1997; Wheeler, 1997; Hildenbrand et al., 2002; McBride et al., 2002b; Odum et al., 2002; Woolery and Street, 2002). No evidence is available to support the intersection of these structures, however. The individual strands of the Fluorspar Area fault complex (FAFC) intersect but do not cross the

Rough Creek fault system (RCFS) (Figure 15; McBride et al., 2002b). Based on seismic-reflection data, Sexton et al. (1986) and Bear et al. (1997) inferred a <40-km-long and ~20-km-wide, Late Precambrian–Early Paleozoic Grayville graben which includes parts of WVFS (dotted lines north of RCFS in Figure 15). Compared to the Reelfoot–Rough Creek rift



▲ **Figure 16.** Ungava Peninsula seismogenic elements. Modified from Bent (1994).

▲ **Figure 15.** Illinois basin seismogenic elements. The dotted lines north of Rough Creek fault system represent the outlines of the Grayville graben. Modified from Hildenbrand *et al.* (2002).

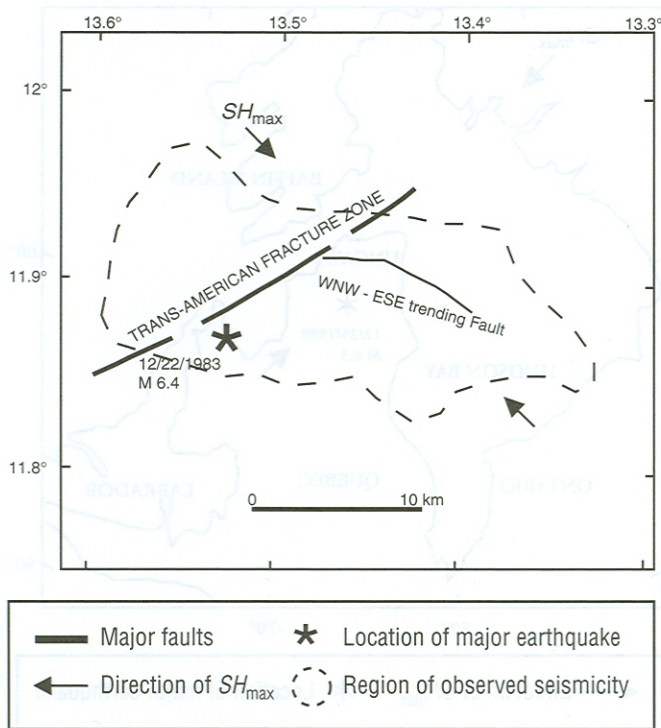
system, the Grayville graben is considerably smaller in cross-section and width (Hildenbrand and Ravat, 1997). Hence in our classification we have considered this region as a non-rift setting. The instrumentally located seismicity lies in the upper and middle crust except for the 9 November 1968  $m_b$  5.5 earthquake, whose hypocentral depth was reported to be  $21.2 \pm 5.4$  km (McBride *et al.*, 2002a). The scarcity of focal mechanisms, precise hypocenters, and information about subsurface geometry of the faults precludes any causal association. The larger earthquakes were located at or near the intersections of these features, particularly the CGFS and CGL (Figure 15). Hildenbrand *et al.* (2002) noted that five of the eight large prehistoric earthquakes known to have occurred within the Illinois basin, including the two largest shocks, clustered at and close to a left-stepping bend in the CGL, as was also reported by Wheeler and Ravat (2002) and Wheeler and Cramer (2002). The buried intrusions in the upper crust are composed of igneous complexes (*e.g.*, the Vincennes Igneous Center), mafic dikes, and some basalt flows (Hildenbrand and Ravat, 1997; Hildenbrand *et al.*, 2002). The majority of the observed seismicity (dashed circle in Figure 15) is uniformly distributed around these intrusions, thus precluding a possible causal association.

One of the largest recent earthquakes in eastern North America was the 25 December 1989  $M_s$  6.3 Ungava earthquake in Canada (Figure 16; Adams *et al.*, 1991; Bent, 1994). The remote region lacks extensive geological and geophysical

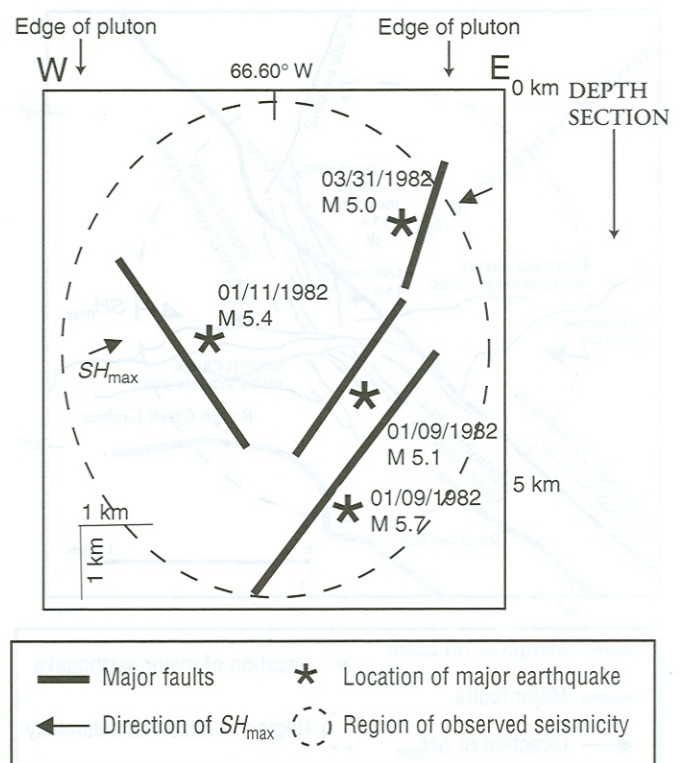
data. Based on waveform modeling studies the mainshock has been postulated to have occurred as two subevents on north-east-southwest- and north-northeast-south-southwest-striking planes (Table 3; Bent, 1994). The former nodal plane is consistent with the  $\sim 38^\circ$  average trend of the surface rupture observed during field studies by Adams *et al.* (1991), but no intersecting faults have been mapped. The presence of buried intrusions, if any, is also not known due to lack of data.

In Guinea, as observed by Neev *et al.* (1982), the north-east-trending Trans-American Fracture Zone, comprising several small and local fractures, passes through the epicentral region of the 22 December 1983  $M$  6.4 earthquake. It intersects a west-northwest-east-southeast-trending fault zone (Talwani and Rajendran, 1991). The mainshock of 22 December 1983 has been teleseismically located to be about 8–10 km from this intersection. Its aftershocks (dashed line in Figure 17), which were located using portable seismographs, lie along the west-northwest-east-southeast-trending fault zone (Figure 17; Langer *et al.*, 1987). The direction of maximum horizontal compression in this region is oriented north-west-southeast (Talwani and Rajendran, 1991), favoring faulting on the west-northwest-east-southeast-trending fault. Given the uncertainties in the location of the mainshock, and well defined alignment of the aftershocks along the west-northwest-east-southeast-trending fault, the mainshock could have been associated with the two intersecting faults.

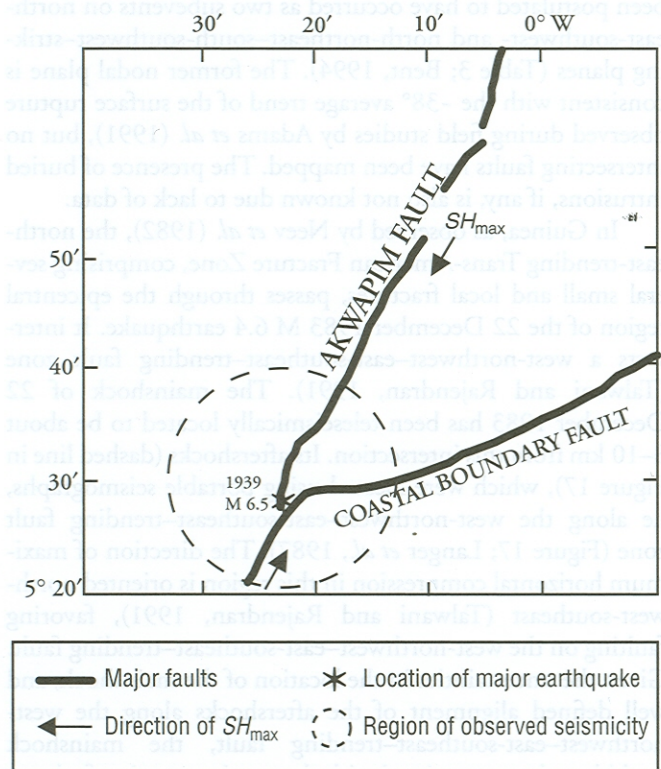
In Ghana the northeast-trending Akwapim Fault cross-cuts the east-northeast-west-southwest-trending Coastal Boundary Fault (Talwani and Rajendran, 1991). This inter-



▲ **Figure 17.** Guinea seismogenic elements. Modified from Langer *et al.* (1987). Trans-American Fracture Zone from Neev *et al.* (1982).



▲ **Figure 19.** Miramichi seismogenic elements. Modified from Hasegawa (1991).



▲ **Figure 18.** Ghana seismogenic elements. Modified from Talwani and Rajendran (1991).

section was the location of the 1939  $M_w$  6.5 Accra earthquake (Figure 18). Focal mechanisms of this earthquake and also several earthquakes during February 1977 and May 1980 (dashed circle in Figure 18) revealed strike-slip and normal faulting (Talwani and Rajendran, 1991). Furthermore, Talwani and Rajendran (1991) observed that Blundell (1976) also identified the intersection of the faults as a zone of weakness, and Bacon and Quaah (1981) noted that a higher level of seismic activity was clustered around this intersection, suggesting a causal association (Figure 18).

Between January and March 1982, four earthquakes with  $M$  5.0–5.7 occurred near Miramichi, Canada. Fault-plane solutions and the hypocentral locations of the aftershocks associated with them define a pair of steeply dipping conjugate faults on the sides of a granitic pluton down to a depth of about 10 km (Figure 19; Hasegawa, 1991; Talwani and Rajendran, 1991). The temporal pattern of the mainshock and aftershocks indicated that the mainshock was initiated at the intersection of the conjugate faults, thus implying its causal association to the intersection (Hasegawa, 1991). The confinement of the seismicity (dashed ellipse in Figure 19) to the edges of the granitic pluton also implies a causal association (Figure 19; Hasegawa, 1991).

In summary, at seven of the eight locations, the possible stress concentrators are either in the form of intersecting faults and/or buried plutons, and none of the locations showed evidence of a rift pillow (Table 3). Five of the eight examined locations have intersecting faults in the vicinity of

the observed seismicity. These are Latur, Illinois Basin, Guinea, Ghana, and Miramichi. Buried plutons are also possible stress concentrators in five of the eight examined locations. These are Latur, western and eastern regions of the Australian craton, Illinois basin, and Miramichi (Table 3).

In the cases of the non-rift-associated intraplate locations such as those examined in this paper, seismicity appears to have longer recurrence periods compared to the rift-associated intraplate locations, as was noted by Johnston (1994). At two intraplate locations where we have good paleoseismological data, Middleton Place Summerville seismic zone in South Carolina and New Madrid seismic zone, the recurrence rates for M 7.0+ earthquakes are ~500 years (Talwani and Schaefer, 2001; Tuttle *et al.*, 2002). In the Charlevoix seismic zone and the Saguenay region, based on paleoseismic records and studies of lake sediments, Ebel and Tuttle (2002) reported average recurrence periods of 75 years and 350–1,000 years respectively for M 6.0+ earthquakes. In the Kachchh rift basin, two M>7.0 earthquakes occurred within 200 years. Cases with documented short recurrence rates ( $\leq 500$  years) occurred within rift basins. The recurrence rates based on paleoseismological data at Tennant Creek, Marryat Creek, and Latur, three locations not associated with rift basins, are of the order of tens of thousands of years (Crone, 1992; Rajendran, 2000). Another intraplate location not associated with a rift basin for which we have an estimate of recurrence rates is the Wabash Valley within the Illinois basin. Here, based on seismicity (Gutenberg-Richter relationship) and paleoseismological data (Obermeier *et al.*, 1991; 1992; 1993), the recurrence rates for M $\geq 6.5$  earthquakes are between 2,600–4,000 years (Frankel *et al.*, 1996).

Thus, from the limited available data we speculate that intraplate earthquakes within the rifts are associated with “characteristic” earthquakes and shorter recurrence periods, whereas those outside the rifts are not and appear to follow the Gutenberg-Richter relationship. As defined by Schwartz and Coppersmith (1984), “characteristic” earthquakes are essentially earthquakes of the same size with a relatively narrow range of magnitudes near the maximum that faults tend to generate. We also note that the largest earthquakes associated with rift-related intraplate regions are larger than those not associated with rifts (Johnston *et al.*, 1994). Rajendran (2000) has also pointed out similar differences. In both cases the common feature is a local stress concentrator which distinguishes it from plate-boundary earthquakes. We are unsure of the exact cause for the difference between the two categories described in this paper. We anticipate that additional high-quality data and three-dimensional modeling will lead to a better understanding of the nature of all categories of intraplate earthquakes.

## DISCUSSION

The objective of this study was to analyze and integrate diverse global geological, geophysical, and seismological data sets to identify common features which can explain the cause

of intraplate earthquakes. These analyses and integration with analytical models of the roles of fault intersections, buried plutons, and rift pillows in localizing stress build-up have allowed us to identify the following features common to the genesis of intraplate earthquakes:

- Intraplate earthquakes occur in pre-existing zones of crustal weakness, the most common of which are failed rift zones, as was originally suggested by Johnston *et al.* (1994).
- Stress build-up and the resulting strain accumulation occur in response to tectonic forces within a localized volume at one or more of the three stress concentrators, *viz.*, fault bends or intersections, buried plutons, and rift pillows.
- One of the intersecting faults was found to be longer and often tens of kilometers in length and oriented optimally with respect to  $SH_{\max}$  for failure.
- Large earthquakes (M $\geq 7.0$ ) associated with intersections and plutons occur at upper crustal depths ( $\leq 15$  km), whereas those associated with rift pillows occur at mid-crustal depths ( $\geq 15$  km).
- Non-rift-associated earthquakes were found to occur only in the Precambrian basement.
- The recurrence intervals for large intraplate earthquakes are longer than for those at plate boundaries.
- The recurrence intervals are shorter for earthquakes within failed rifts as compared to those associated with structures outside rifts.
- Any mechanical model proposed for the generation of intraplate earthquakes will have to address these observations. ☒

## ACKNOWLEDGMENTS

We thank the reviewers, Drs. Thomas G. Hildenbrand, Susan E. Hough, and Russell L. Wheeler for their critical and constructive comments.

## REFERENCES

- Adams, J., R. J. Wetmiller, H. S. Hasegawa, and J. Drysdale (1991). The first surface faulting from a historical intraplate earthquake in North America, *Nature* **352**, 617–619.
- Andrews, D. J. (1994). Fault geometry and earthquake mechanics, *Annali Geofisica* **37**, 1,341–1,348.
- Andrews, D. J. (1989). Mechanics of fault junctions, *Journal of Geophysical Research* **94**, 9,389–9,397.
- Assumpcao, M. and G. Suarez (1988). Source mechanisms of moderate-size earthquakes and stress orientation in mid-plate South America, *Geophysical Journal* **92**, 253–267.
- Atchuta Rao, D., H. V. Ram Babu, G. D. J. Sivakumar Sinha (1992). Crustal structure associated with Gondwana graben across the Narmada-Son lineament in India: An inference from aeromagnetism, *Tectonophysics* **212**, 163–172.
- Barstow, N. L., K. G. Brill, Jr., O. W. Nuttli, and P. W. Pomeroy (1981). *An Approach to Seismic Zonation for Siting Nuclear Electric Power Generating Facilities in the Eastern United States*, NUREG/CR-1577, U.S. Nuclear Regulatory Commission.

- Basham, P. W., D. A. Forsyth, and R. J. Wetmiller (1977). The seismicity of northern Canada, *Canadian Journal of Earth Sciences* **14**, 1,646–1,667.
- Bear, G. W., J. A. Rupp, and A. J. Rudman (1997). Seismic interpretation of the deep structure of the Wabash Valley fault system, *Seismological Research Letters* **68**, 624–640.
- Bent, A. L. (1992). A Re-examination of the 1925 Charlevoix, Quebec, Earthquake, *Bulletin of the Seismological Society of America* **82**, 2,097–2,113.
- Bent, A. L. (1994). The 1989 ( $M_s$  6.3) Ungava, Quebec, earthquake: A complex intraplate event, *Bulletin of the Seismological Society of America* **84**, 1,075–1,088.
- Biswas, S. K. (1987). Regional tectonic framework, structure and evolution of the western marginal basins of India, *Tectonophysics* **135**, 307–327.
- Biswas, S. K. (1982). Rift basins in western margin of India and their hydrocarbon prospects with special reference to Kutch basin, *American Association of Petroleum Geologists Bulletin* **66**, 1,497–1,513.
- Biswas, S. K. and K. N. Khattri (2002). A geological study of earthquakes in Kutch, Gujarat, India, *Journal of the Geological Society of India* **60**, 131–142.
- Bowman, J. R. (1991). Geodetic evidence for conjugate faulting during the 1988 Tennant Creek, Australia earthquake sequence, *Geophysical Journal International* **107**, 47–56.
- Bowman, J. R. (1992). The 1988 Tennant Creek, Northern Territory, earthquakes: A synthesis, *Australian Journal of Earth Science* **39**, 651–669.
- Bowman, J. R. and J. W. Dewey (1991). Relocation of teleseismically recorded earthquakes near Tennant Creek, Australia: Implications for midplate seismogenesis, *Journal of Geophysical Research* **96**, 11,973–11,979.
- Bowman, J. R., G. Gibson, and T. Jones (1990). Aftershocks of the 1988 January 22 Tennant Creek, Australia intraplate earthquakes: Evidence for a complex thrust-fault geometry, *Geophysical Journal International* **100**, 87–97.
- Campbell, D. L. (1978). Investigation of the stress-concentration mechanism for intraplate earthquakes, *Geophysical Research Letters* **5**, 477–479.
- Choy, G. L. and J. R. Bowman (1990). Rupture process of a multiple main shock sequence: Analysis of teleseismic, local and field observations of the Tennant Creek, Australia earthquakes, *Journal of Geophysical Research* **95**, 6,867–6,882.
- Chung, W. Y. (1993). Source parameters of two rift-associated intraplate earthquakes in peninsular India: The Bhadrachalam earthquake of April 13, 1967 and the Broach earthquake of March 23, 1970, *Tectonophysics* **225**, 219–230.
- Chung, W. Y. and H. Gao (1995). Source parameters of the Anjar earthquake of July 21, 1956, India, and its seismotectonic implications for the Kutch rift basin, *Tectonophysics* **242**, 281–292.
- Costain, J. K., G. A. Bollinger, and J. A. Speer (1987). Hydroseismicity: A hypothesis for the role of water in the generation of intraplate seismicity, *Seismological Research Letters* **58**, 41–64.
- Crone, A. J., M. N. Machette, and J. R. Bowman (1992). *Geologic Investigations of the 1988 Tennant Creek, Australia, Earthquakes: Implications for Paleoseismicity in Stable Continental Regions*, U.S. Geological Survey Bulletin 2032-A, 51 pp.
- Denham, D. (1988). Australian seismicity—The puzzle of the not-so-stable continent, *Seismological Research Letters* **59**, 235–240.
- Deverchere, J., F. Houdry, N. V. Solonenko, A. V. Solonenko, and V. A. Sankov (1993). Seismicity, active faults and stress field of the north Muya Region, Baikal Rift: New insights on the rheology of extended continental lithosphere, *Journal of Geophysical Research* **98**, 19,895–19,912.
- Deverchere, J., C. Petit, N. Gileva, N. Radziminovitch, V. Melnikova, and V. San'kov (2001). Depth distribution of earthquakes in the Baikal rift system and its implications for the rheology of the lithosphere, *Geophysical Journal International* **146**, 714–730.
- Du Berger, R., D. W. Roy, M. Lamontagne, G. Woussen, R. G. North, and R. J. Wetmiller (1991). The Saguenay (Quebec) earthquake of November 25, 1988: Seismologic data and geologic setting, *Tectonophysics* **186**, 59–74.
- Ebel, J. E. (1996). The seventeenth century seismicity of northeastern North America, *Seismological Research Letters* **67**, 51–68.
- Ebel, J. E. and M. Tuttle (2002). Earthquakes in the eastern Great Lakes Basin from a regional perspective, *Tectonophysics* **353**, 17–30.
- Frankel, A., T. B. Mueller, D. Perkins, E. V. Leyendecker, N. Dickman, S. Hanson, and M. Hopper (1996). *National Seismic Hazard Maps: Documentation June 1996*, U.S. Geological Survey Open-File Report 96-532, 70 pp.
- Gaulon, R., J. Chorowicz, G. Vidal, B. Romanowicz, and G. Roullet (1992). Regional geodynamic implications of the May–July 1990 earthquake sequence in southern Sudan, *Tectonophysics* **209**, 87–103.
- Giardini, D. and L. Beranzoli (1992). Waveform modeling of the May 20, 1990 Sudan earthquake, *Tectonophysics* **209**, 105–114.
- Girdler, R. W. and D. A. McConnell (1994). The 1990 to 1991 Sudan earthquake sequence and the extent of the East African Rift system, *Science* **264**, 67–70.
- Goodacre, A. K. and H. S. Hasegawa (1980). Gravitationally induced stresses at structural boundaries, *Canadian Journal of Earth Sciences* **17**, 1,286–1,291.
- Gordon, F. R. and J. D. Lewis (1980). The Meckering and Calingiri earthquakes of October 1968 and March 1970, *Geological Survey of Western Australia Bulletin* **126**, 1–229.
- Grollmund, B. and M. D. Zoback (2001). Did deglaciation trigger intraplate seismicity in the New Madrid seismic zone?, *Geology* **29**, 175–178.
- Gupta, H. K., R. K. Chadha, M. N. Rao, B. L. Narayana, P. Mandal, M. Ravi Kumar, and N. Kumar (1997). The Jabalpur Earthquake of May 22, 1997, *Journal of the Geological Society of India* **50**, 85–91.
- Haddon, R. A. W. (1995). Modeling of source rupture characteristics for the Saguenay earthquake of November 1988, *Bulletin of the Seismological Society of America* **85**, 525–551.
- Hasegawa, H. S. (1991). Four seismogenic environments in eastern Canada, *Tectonophysics* **186**, 3–17.
- Hildenbrand, T. G., A. Griscom, R. S. Van Schumus and W. Stuart (1996). Quantitative investigations of the Missouri gravity low—A possible expression of a large Late Precambrian batholith intersecting the New Madrid seismic zone, *Journal of Geophysical Research* **101**, 21,921–21,942.
- Hildenbrand, T. G. and J. D. Hendricks (1995). Geophysical setting of the Reelfoot Rift and relations between rift structures and the New Madrid seismic zone, U.S. Geological Survey Professional Paper 1528-E, 1–30.
- Hildenbrand, T. G., J. H. McBride, and D. Ravat (2002). The Commerce geophysical lineament and its possible relation to Mesoproterozoic igneous complexes and large earthquakes in the central Illinois basin, *Seismological Research Letters* **73**, 640–659.
- Hildenbrand, T. G. and D. Ravat (1997). Geophysical setting of the Wabash Valley fault system, *Seismological Research Letters* **68**, 567–585.
- Hildenbrand, T. G., W. D. Stuart, and P. Talwani (2001). Geologic structures related to New Madrid earthquakes near Memphis, Tennessee, based on gravity and magnetic interpretations, *Engineering Geology* **62**, 105–121.
- Hough, S. E., J. G. Armbruster, L. Seeber, and J. F. Hough (2000). On the Modified Mercalli intensities and magnitudes of the 1811–1812 New Madrid earthquakes, *Journal of Geophysical Research* **105**, 23,839–23,864.

- Illies, J. H. (1982). Der Hohenzollern Graben und Intraplatten-Seismizität infolge Vergitterung lamellarer Scherung mit einer Riftstruktur, *Oberrhein. Geol. Abh.* **31**, 47–78.
- Johnston, A. C. (1996). Seismic moment assessment of earthquakes in stable continental regions, II: New Madrid 1811–1812, Charleston 1886 and Lisbon 1755, *Geophysical Journal International* **126**, 314–344.
- Johnston, A. C. (1989). The seismicity of “stable” continental interiors, in S. Gregersen and P. W. Basham (editors), *Earthquakes at North-Atlantic Passive Margins: Neotectonics and Post-Glacial Rebound*, NATO ASI Series C, Mathematical and Physical Sciences, 563–579.
- Johnston, A. C., K. J. Coppersmith, L. R. Kanter, and C. A. Cornell (1994). *The Earthquakes of Stable Continental Regions: Assessment of Large Earthquake Potential*, EPRI Report TR-102261, J. F. Schneider, editor. Palo Alto, CA: Electric Power Research Institute, 309 pp.
- Johnston, A. C. and E. S. Schweig (1996). The enigma of the New Madrid earthquakes of 1811–1812, *Annual Review of Earth and Planetary Sciences* **24**, 339–384.
- Kane, M. F. (1977). Correlation of major eastern earthquake centers with mafic/ultramafic basement masses, in D. W. Rankin (editor), *Studies Related to the Charleston, South Carolina, Earthquake of 1886—A Preliminary Report*, U.S. Geological Survey Professional Paper 1028, 199–204.
- Kar, A. (1993). Neotectonic influences on morphological variations along the coastline of Kachchh, India, *Geomorphology* **8**, 199–219.
- Kayal, J. R. (2000). Seismotectonic study of the two recent SCR earthquakes in central India, *Journal of the Geological Society of India* **55**, 123–138.
- Kayal, J. R., R. De, B. Das, and S. N. Chowdhury (1996). Aftershock monitoring and focal mechanism studies, *Geological Survey of India Special Publication* **37**, 165–185.
- Kayal, J. R., R. De, S. Ram, B. V. Srirama, and S. G. Gaonkar (2002). Aftershocks of the 26 January, 2001 Bhuj earthquake in western India and its seismotectonic implications, *Journal of the Geological Society of India* **59**, 395–417.
- Kenner, S. J. and P. Segall (2000). A mechanical model for intraplate earthquakes: Application to the New Madrid seismic zone, *Science* **289**, 2329–2332.
- King, G. and J. Nabelek (1985). Role of fault bends in the initiation and termination of earthquake rupture, *Science* **228**, 984–987.
- King, G. C. P. (1986). Speculations on the geometry of the initiation and termination processes of earthquake rupture and its relation to morphological and geological structure, *Pure and Applied Geophysics* **124**, 567–585.
- Kolata, D. R. and T. G. Hildenbrand (1997). Structural underpinnings and neotectonics of the southern Illinois basin: An overview, *Seismological Research Letters* **68**, 499–510.
- Kumar, P., H. C. Tewari, and G. Khandekar (2000). An anomalous high-velocity layer at shallow crustal depths in the Narmada zone, India, *Geophysical Journal International* **142**, 95–107.
- Kumarapeli, P. S. (1993). A plume-generated segment of the rifted margin of Laurentia, Southern Canadian Appalachians, seen through a completed Wilson Cycle, *Tectonophysics* **219**, 47–55.
- Lamontagne, M. and G. Ranalli (1997). Faults and spatial clustering of earthquakes near La Malbaie, Charlevoix seismic zone, Canada, *Seismological Research Letters* **68**, 337–352.
- Langer, C. J., M. G. Bonilla, and G. A. Bollinger (1987). Aftershocks and surface faulting associated with the intraplate Guinea, West Africa, earthquake of 22 December 1983, *Bulletin of the Seismological Society of America* **77**, 1,579–1,601.
- Langston, C. A. (1987). Depth of faulting during the 1968 Meckering, Australia, earthquake sequence determined from waveform analysis of local seismograms, *Journal of Geophysical Research* **92**, 11,561–11,574.
- Lemeille, F., M. Cushing, D. Carbon, B. Grellet, T. Bitterli, C. Flehoc, and C. Innocent (1999). Co-seismic ruptures and deformations recorded by speleothems in the epicentral zone of the Basel earthquake, *Geodinamica Acta* **12**, 179–191.
- Long, L. T. and J. W. Champion, Jr. (1977). Bouguer gravity map of the Summerville–Charleston, South Carolina epicentral zone and tectonic implications, in D. W. Rankin (editor), *Studies Related to the Charleston, South Carolina, Earthquake of 1886—A Preliminary Report*, U.S. Geological Survey Professional Paper 1028, 151–166.
- Marple, R. T. and P. Talwani (2000). Evidence for a buried fault system in the coastal plain of the Carolinas and Virginia—Implications for neotectonics in the southeastern United States, *Bulletin of the Geological Society of America* **112**, 200–220.
- Marshak, S. and T. Paulsen (1997). Structural style, regional distribution, and seismic implications of midcontinent fault-and-fold zones, United States, *Seismological Research Letters* **68**, 511–520.
- Mayer, G., P. M. Mai, T. Plenefisch, H. Echlter, E. Luschen, V. Wehrle, B. Muller, K.–P. Bonjer, C. Prodehl, and K. Fuchs (1997). The deep crust of the Southern Rhine graben: Reflectivity and seismicity as images of dynamic processes, *Tectonophysics* **275**, 15–40.
- McBride, J. H., T. G. Hildenbrand, W. J. Stephenson, and C. J. Potter (2002a). Interpreting the earthquake source of the Wabash Valley seismic zone (Illinois, Indiana, and Kentucky) from seismic-reflection, gravity, and magnetic-intensity data, *Seismological Research Letters* **73**, 660–686.
- McBride, J. H., K. D. Nelson, and L. D. Brown (1989). Evidence and implications of an extensive early Mesozoic rift basin and basalt/diabase sequence beneath the southeast Coastal Plain, *Geological Society of America Bulletin* **101**, 512–520.
- McBride, J. H., W. J. Nelson, and W. J. Stephenson (2002b). Integrated geological and geophysical study of Neogene and Quaternary-age deformation in the northern Mississippi embayment, *Seismological Research Letters* **73**, 597–627.
- McKeown, F. A. (1978). Hypothesis: Many earthquakes in the central and southeastern United States are causally related to mafic intrusive bodies, *Journal Research U.S. Geological Survey* **6**, 41–50.
- Meghraoui, M., B. Delouis, M. Ferry, D. Giardini, P. Huggenberger, I. Spotke, and M. Granet (2001). Active normal faulting in the Upper Rhine graben and paleoseismic identification of the 1356 Basel earthquake, *Science* **293**, 2,070–2,073.
- Mishra, D. C. and S. B. Gupta (1998). Mid-continent gravity “high” and seismic activities in central India, *Current Science* **74**, 702–705.
- Mishra, D. C., S. B. Gupta, M. B. S. V. Rao, M. Venkatarayudu, and G. Laxman (1987). Godavari basin—A geophysical study, *Journal of the Geological Society of India* **30**, 469–476.
- Mishra, D. C. and S. Ravi Kumar (1998). Characteristics of faults associated with Narmada Son lineament and rock types in Jabalpur sector, *Current Science* **75**, 308–310.
- Mishra, D. C., V. M. Tiwari, S. B. Gupta, and M. B. S. Vyaghreswara Rao (1998). Anomalous mass distribution in the epicentral area of Latur earthquake, India, *Current Science* **74**, 469–472.
- Nabelek, J., W. P. Chen, and Ye (1987). The Tangshan earthquake sequence and its implications for the evolution of the North China basin, *Journal of Geophysical Research* **92**, 12,615–12,628.
- Neev, D., J. K. Hall, and J. M. Saul (1982). The Pelusium megashear system across Africa and associated lineament swarms, *Journal of Geophysical Research* **87**, 1,015–1,030.
- Nunn, J. A. and J. R. Aires (1988). Gravity anomalies and flexure of the lithosphere at the Middle Amazon basin, Brazil, *Journal of Geophysical Research* **93**, 415–428.
- Obermeier, S. F., N. K. Bleuer, P. J. Munson, W. S. Martin, K. M. McWilliams, D. A. Tabaczynski, J. K. Odum, M. Rubin, and D. L. Eggert (1991). Evidence of strong earthquake shaking in the lower Wabash Valley from prehistoric liquefaction features, *Science* **251**, 1,061–1,063.

- Obermeier, S. F., J. R. Martin, A. D. Frankel, T. L. Youd, P. J. Munson, C. A. Munson, and E. C. Pond (1993). *Liquefaction Evidence for One or More Strong Holocene Earthquakes in the Wabash Valley of Southern Indiana and Illinois, with a Preliminary Estimate of Magnitude*, U.S. Geological Survey Professional Paper 1536, 27 pp.
- Obermeier, S. F., P. J. Munson, C. A. Munson, J. R. Martin, A. D. Frankel, T. L. Youd, and E. C. Pond (1992). Liquefaction evidence for strong Holocene earthquake(s) in the Wabash Valley of Indiana-Illinois, *Seismological Research Letters* **63**, 321–335.
- Odum, J. K., W. J. Stephenson, R. A. Williams, J. A. Devera, and J. R. Staub (2002). Near-surface faulting and deformation overlying the Commerce geophysical lineament in southern Illinois, *Seismological Research Letters* **73**, 687–697.
- Pollitz, F. F., L. Kellogg, and R. Burgmann (2001). Sinking mafic body in a reactivated lower crust: A mechanism for stress concentration at the New Madrid seismic zone, *Bulletin of the Seismological Society of America* **91**, 1,882–1,897.
- Rajendran, C. P. (2000). Using geologic data for earthquake studies: A perspective from peninsular India, *Current Science* **79**, 1251–1258.
- Rajendran, C. P., K. Rajendran, and B. John (1996). The 1993 Killari (Latur), central India, earthquake: An example of fault reactivation in the Precambrian crust, *Geology* **24**, 651–654.
- Rajendran, K. and C. P. Rajendran (1998). Characteristics of the 1997 Jabalpur earthquake and their bearing on its mechanism, *Current Science* **74**, 168–174.
- Rajendran, K. and C. P. Rajendran (1999). Seismogenesis in the stable continental interiors: An appraisal based on two examples from India, *Tectonophysics* **305**, 355–370.
- Rao, G. V. and R. U. M. Rao (1983). Heat flow in Indian Gondwana basins and heat production of their basement rocks, *Tectonophysics* **91**, 105–117.
- Rao Ramalingeswara, B. and P. Rao Sitapathi (1984). Historical seismicity of peninsular India, *Bulletin of the Seismological Society of America* **74**, 2,519–2,533.
- Ravat, D. N., L. W. Braile, and W. J. Hinze (1987). Earthquakes and plutons in the mid-continent—Evidence from the Bloomfield pluton, New Madrid rift complex, *Seismological Research Letters* **58**, 41–52.
- Rhea, S. and R. L. Wheeler (1995). Map showing synopsis of seismotectonic features in the vicinity of New Madrid, Missouri, U.S. Geological Survey Miscellaneous Investigations Series, I-2521.
- Schneider, G. (1979). The earthquake in the Swabian Jura of 16 November 1911 and present concepts of seismotectonics, *Tectonophysics* **53**, 279–288.
- Schwartz, D. P. and K. J. Coppersmith (1984). Fault behavior and characteristic earthquakes: Examples from the Wasatch and San Andreas Fault zones, *Journal of Geophysical Research* **89**, 5,681–5,698.
- Seeber, L., G. Ekstrom, S. K. Jain, C. V. R. Murty, N. Chandak, and J. G. Armbruster (1996). The 1993 Killari earthquake in central India: A new fault in Mesozoic basalt flows?, *Journal of Geophysical Research* **101**, 8,543–8,560.
- Sexton, J. L., L. W. Braile, W. J. Hinze, and M. J. Campbell (1986). Seismic reflection profiling studies of a buried Precambrian rift beneath the Wabash Valley fault zone, *Geophysics* **51**, 640–660.
- Shedlock, K. M., J. Baranowski, X. Weiwen, and H. X. Liang (1987). The Tangshan aftershock sequence, *Journal of Geophysical Research* **92**, 2,791–2,803.
- Simmons, G., R. Wang, and H. Illfelder (1976). The Ossipee Mountains, New Hampshire: Earthquakes and a stress model, in Boston Edison Company, Pilgrim Unit 2: Report Submitted to Nuclear Regulatory Commission Pursuant to Licensing of Pilgrim Unit 2, B1-1–B1-15.
- Singh, A. P. and R. Meissner (1995). Crustal configuration of the Narada-Tapti region (India) from gravity studies, *Journal of Geodynamics* **20**, 111–127.
- Stein, S., N. Sleep, R. J. Geller, S. C. Wang, and G. C. Kroeger (1979). Earthquakes along the passive margin of eastern Canada, *Geophysical Research Letters* **6**, 537–540.
- Stuart, W. D., T. G. Hildenbrand, and R. W. Simpson (1997). Stressing of the New Madrid seismic zone by a lower crust detachment fault, *Journal of Geophysical Research* **102**, 27,623–27,633.
- Sykes, L. R. (1978). Intraplate seismicity, reactivation of preexisting zones of weakness, alkaline magmatism, and other tectonism post-dating continental fragmentation, *Reviews of Geophysics and Space Physics* **16**, 621–688.
- Talwani, P. (1989). Characteristic features of intraplate earthquakes and the models proposed to explain them, in S. Gregersen and P. W. Basham (editors), *Earthquakes at North-Atlantic Passive Margins: Neotectonics and Post-Glacial Rebound*, NATO ASI Ser. C, Mathematical and Physical Sciences, 563–579.
- Talwani, P. (1985). Current thoughts on the cause of the Charleston, South Carolina earthquakes, *South Carolina Geology* **29**, 19–38.
- Talwani, P. (1982). Internally consistent pattern of seismicity near Charleston, South Carolina, *Geology* **10**, 654–658.
- Talwani, P. (1988). The intersection model for intraplate earthquakes, *Seismological Research Letters* **59**, 305–310.
- Talwani, P. (2000). Macroscopic effects of the 1886 Charleston earthquake, *A Compendium of Field Trips of South Carolina Geology with Emphasis on the Charleston, South Carolina Area*, South Carolina Department of Natural Resources Geological Survey, 1–6.
- Talwani, P. and S. D. Acree (1984). Pore pressure diffusion and the mechanism of reservoir induced seismicity, *Journal of Pure and Applied Geophysics* **122**, 947–965.
- Talwani, P., D. C. Amick, and R. Logan (1979). A model to explain the intraplate seismicity in the South Carolina Coastal Plain, *Eos, Transactions of the American Geophysical Union* **60**, 311.
- Talwani, P. and A. Gangopadhyay (2001). Tectonic framework of the Kachchh earthquake of 26 January 2001, *Seismological Research Letters* **72**, 336–345.
- Talwani, P. and K. Rajendran (1991). Some seismological and geometric features of intraplate earthquakes, *Tectonophysics* **186**, 19–41.
- Talwani, P. and W. T. Schaeffer (2001). Recurrence rates of large earthquakes in the South Carolina Coastal Plain based on paleoliquefaction data, *Journal of Geophysical Research* **106**, 6,621–6,642.
- Talwani, P. and R. E. Weems (2001). Neotectonic activity in the Charleston, South Carolina region, *Geological Society of America Abs. Prog.* **33**, 346.
- ten Brink, U. S. and M. H. Taylor (2002). Crustal structure of central Lake Baikal: Insights into intracontinental rifting, *Journal of Geophysical Research* **107**, ETG 2-1–2-15.
- Thybo, H., E. Perchuc, and S. Zhou (2000). Intraplate earthquakes and a seismically defined lateral transition in the upper mantle, *Geophysical Research Letters* **27**, 3,953–3,956.
- Turnovsky, J. and G. Schneider (1982). The seismotectonic character of the September 3, 1978, Swabian Jura earthquake series, *Tectonophysics* **83**, 151–162.
- Tuttle, M. P., E. S. Schweig, J. D. Sims, R. H. Lafferty, L. W. Wolf, and M. L. Haynes (2002). The earthquake potential of the New Madrid seismic zone, *Bulletin of the Seismological Society of America* **92**, 2,080–2,089.
- Valdiya, K. S. (1973). Tectonic framework of India: A review and interpretation of recent structural and tectonic studies, *Geophysical Research Bulletin* **11**, 79–114.
- Van Arsdale, R. B., K. I. Kelson, and C. H. Lumsden (1995). Northern extension of the Tennessee Reelfoot scarp into Kentucky and Missouri, *Seismological Research Letters* **66**, 57–62.
- Van Arsdale, R. B., J. Purser, W. Stephenson, and J. Odum (1998). Faulting along the southern margin of Reelfoot Lake, Tennessee, *Bulletin of the Seismological Society of America* **88**, 131–139.
- Wheeler, R. L. (1997). Boundary separating the seismically active Reelfoot Rift from the sparsely seismic Rough Creek graben, Kentucky and Illinois, *Seismological Research Letters* **68**, 586–598.

- Wheeler, R. L. and C. H. Cramer (2002). Updated seismic hazard in the southern Illinois Basin: Geological and geophysical foundations for use in the 2002 USGS National Seismic Hazard Maps, *Seismological Research Letters* **73**, 776–791.
- Wheeler, R. L. and D. Ravat (2002). Introduction: Seismicity, Quaternary faulting, and seismic hazard, *Seismological Research Letters* **73**, 590–596.
- Woolery, E. W. and R. Street (2002). Quaternary fault reactivation in the Fluorspar area fault complex of western Kentucky: Evidence from shallow SH-wave reflection profiles, *Seismological Research Letters* **73**, 628–639.
- Zoback, M. L. (1992). Stress field constraints on intraplate seismicity in eastern North America, *Journal of Geophysical Research* **97**, 11,761–11,782.
- Zoback, M. L. and R. M. Richardson (1996). Stress perturbation associated with the Amazonas and other ancient continental rifts, *Journal of Geophysical Research* **101**, 5,459–5,475.
- Zoback, M. L., M. D. Zoback, J. Adams, M. Assumpção, S. Bell, E. A. Bergman, P. Blumling, N. R. Brereton, D. Denham, J. Ding, K. Fuchs, N. Gay, S. Gregersen, H. K. Gupta, A. Gvishiani, K. Jacob, R. Klein, P. Knoll, M. Magee, J. L. Mercier, B. C. Muller, C. Paquin, K. Rajendran, O. Stephansson, G. Suarez, M. Suter, A. Udías, Z. H. Xu, and M. Zhizhin (1989). Global patterns of tectonic stress, *Nature* **341**, 291–298.

*Department of Geological Sciences*  
*University of South Carolina*  
*Columbia, SC 29208*  
*abhijit@seis.sc.edu*  
*talwani@geol.sc.edu*